https://ntrs.nasa.gov/search.jsp?R=19760007486 2020-03-22T18:19:13+00:00Z

General Disclaimer

One or more of the Following Statements may affect this Document

- This document has been reproduced from the best copy furnished by the organizational source. It is being released in the interest of making available as much information as possible.

- This document may contain data, which exceeds the sheet parameters. It was furnished in this condition by the organizational source and is the best copy available.

- This document may contain tone-on-tone or color graphs, charts and/or pictures, which have been reproduced in black and white.

- This document is paginated as submitted by the original source.

- Portions of this document are not fully legible due to the historical nature of some of the material. However, it is the best reproduction available from the original submission.

Produced by the NASA Center for Aerospace Information (CASI)

NASA CR-
144638

N76-14574
Unclas
G3/43 05650
(NASA-CR-144638) SOIL MOISTURE DETECTION FROM RADAR IMAGERY OF THE PHOENIX, ARIZONA TEST SITE (Kansas Univ. Center for Research, Inc.) 40 p HC $4.00 CSCL 17I

SOIL MOISTURE DETECTION FROM RADAR IMAGERY OF THE PHOENIX, ARIZONA TEST SITE

Remote Sensing Laboratory
RSL Technical Report 264-4

Josef Cihlar
Fawwaz Ulaby
Raymond Mueller

RECEIVED
NASA STI FACILITY
INPUT BRANCH

June, 1975

Supported by:

NATIONAL AERONAUTICS AND SPACE ADMINISTRATION
Lyndon B. Johnson Space Center
Houston, Texas 77058

CONTRACT NAS 9-14052

THE UNIVERSITY OF KANSAS CENTER FOR RESEARCH, INC.
2291 Irving Hill Drive—Campus West Lawrence, Kansas 66045

TABLE OF CONTENTS

LIST OF ILLUSTRATIONS

LIST OF ILLUSTRATIONS (CONTINUED)

ABSTRACT

The Environmental Research Institute of Michigan (ERIM) dual-polarization X- and L-band radar was flown on April 5, 1974 to acquire radar imagery over the Phoenix (Arizona) test site. Being L-shaped, the test site was covered by two passes, a North-South pass and an East-West pass. The purpose of the mission was to investigate the radar response to soil moisture variations. Soil moisture samples and ground truth information were collected by field crews from about 90 bare fields. No detailed analysis of the X-band digitized data was possible due to the narrow dynamic range produced by the digitization process at ERIM. In its present configuration, the ERIM radar does not have accurately measured antenna patterns. In view of this limitation, the analysis of the L-band data was performed separately for each of several strips along the flight line, where each strip corresponds to a narrow angle of incidence range. For the NS pass, good correlation between the radar return and moisture content was observed for each of the two nearest (to nadir) angular ranges: 42.8°-47.1° and 47.1°-50.7°, although the number of fields in each of these ranges was only 5. At the higher angular ranges, no correlation was observed. Due to misalignment between the flight path of the EW pass and the test site, the above procedure was not applied. The findings reported herein stress the importance of radar calibration, proper choice of the dynamic range of interest in the digitization process, and the need for angles of incidence closer to nadir than was provided by the ERIM radar mission over the Phoenix test site.

1. INTRODUCTION

As part of the Joint Soil Moisture Experiment, a remote sensing mission involving active and passive microwave sensors as well as supporting visible and infrared sensors was undertaken on April 5, 1974 over the Phoenix (Arizona) test site. The objective of the experiment was to acquire microwave data and corresponding ground information necessary for establishing the response of airborne microwave sensors to soil moisture of bare and vegetated fields. The purpose of this report is to describe the data, analyses, and results pertaining to the relationship between the active microwave (radar) measurements and ground parameters, particularly soil moisture. The radar data were acquired by the Environmental Research Institute of Michigan (ERIM) synthetic aperture imaging radar operating at 1.304 GHz (L-band) and 9.375 GHz (X-band). At each of the two frequencies HH and HV polarization configurations were recorded.

2. TEST SITE

The Phoenix test site consisted of two parts positioned in the North-South and East-West directions and located West and South of Phoenix, respectively. The NS section, shown in Map 1, extended 0.5 mile on either side of 91st Avenue (longitude 112°15.04'W) and from 2 miles S of Baseline Road (latitude 33°20.7'N) to 2 miles N of Sun City (latitude 33°38'N). The EW section (shown in Map 2) was formed by a 1-mile wide strip centered on Guadalupe Road and positioned between 91st Avenue (latitude 33°21.98'N, longitude 112°15'W0 and the Maricopa/Pinal County line (latitude 33°21.98'N, longitude 111°35'). The test site was relatively flat, in part due to artificial leveling of the soil surface. Loams and clay loams were the main soil textural categories represented. The majority of the land within the test site was used for crop production although other land use categories (built-up land, natural vegetation, etc.) were also present. Individual fields were large and of uniform shape. An extensive channel network serves for transporting irrigation water to individual fields.

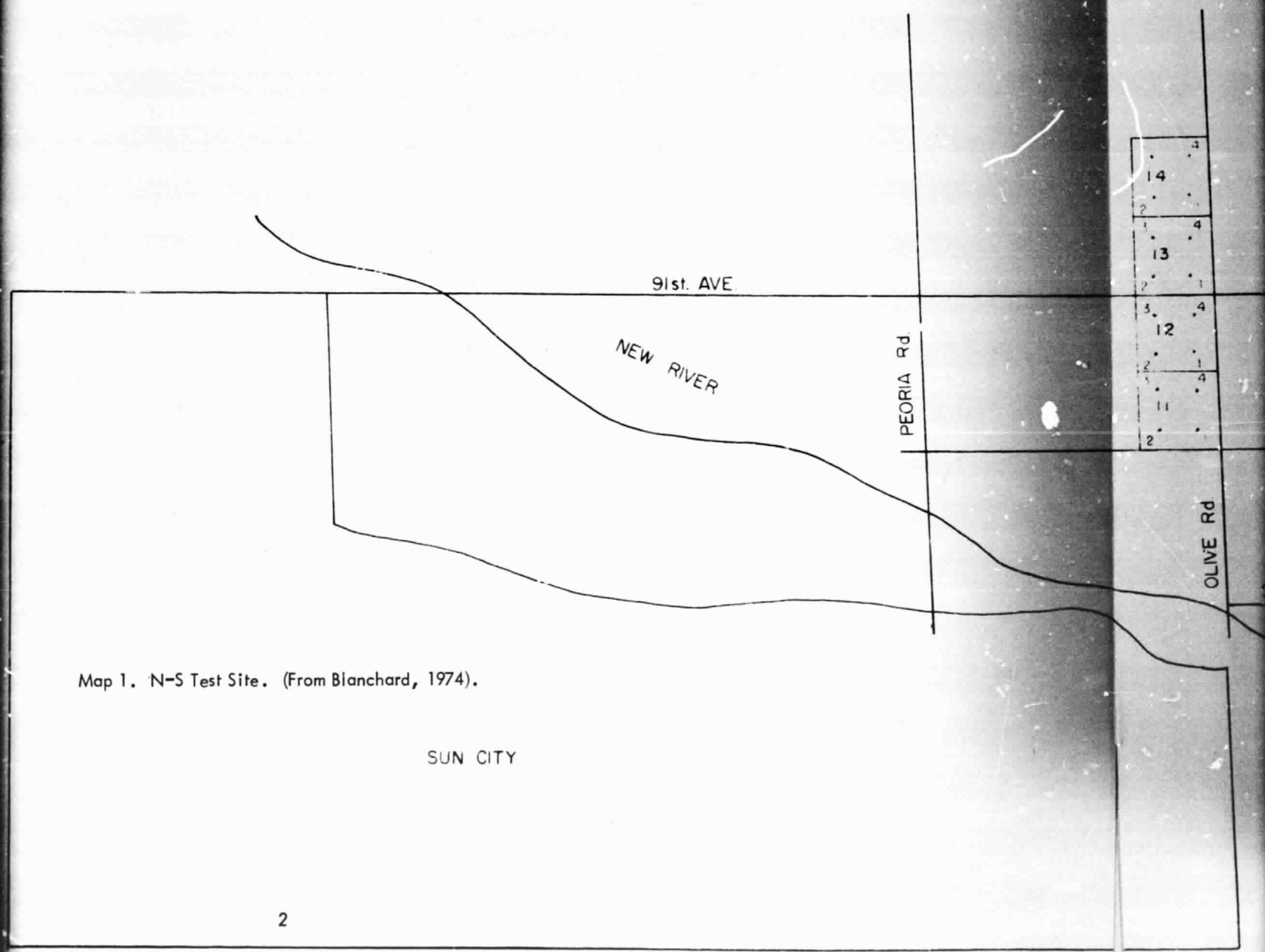

Map 1. N-S Test Site. (From Blanchard, 1974).

SUN CITY

FOLDOUT FRAME

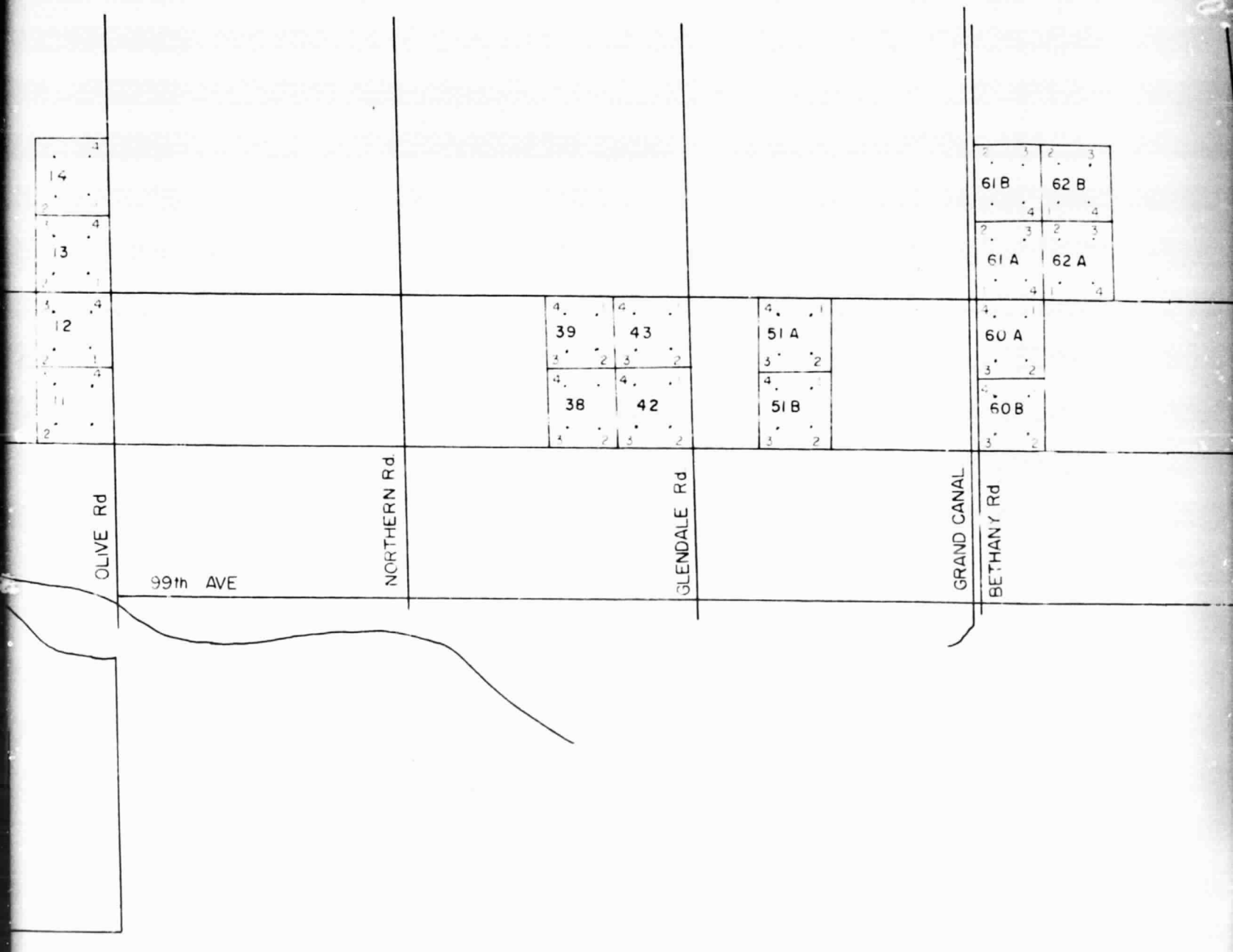

FOLDOUT FRAME 2

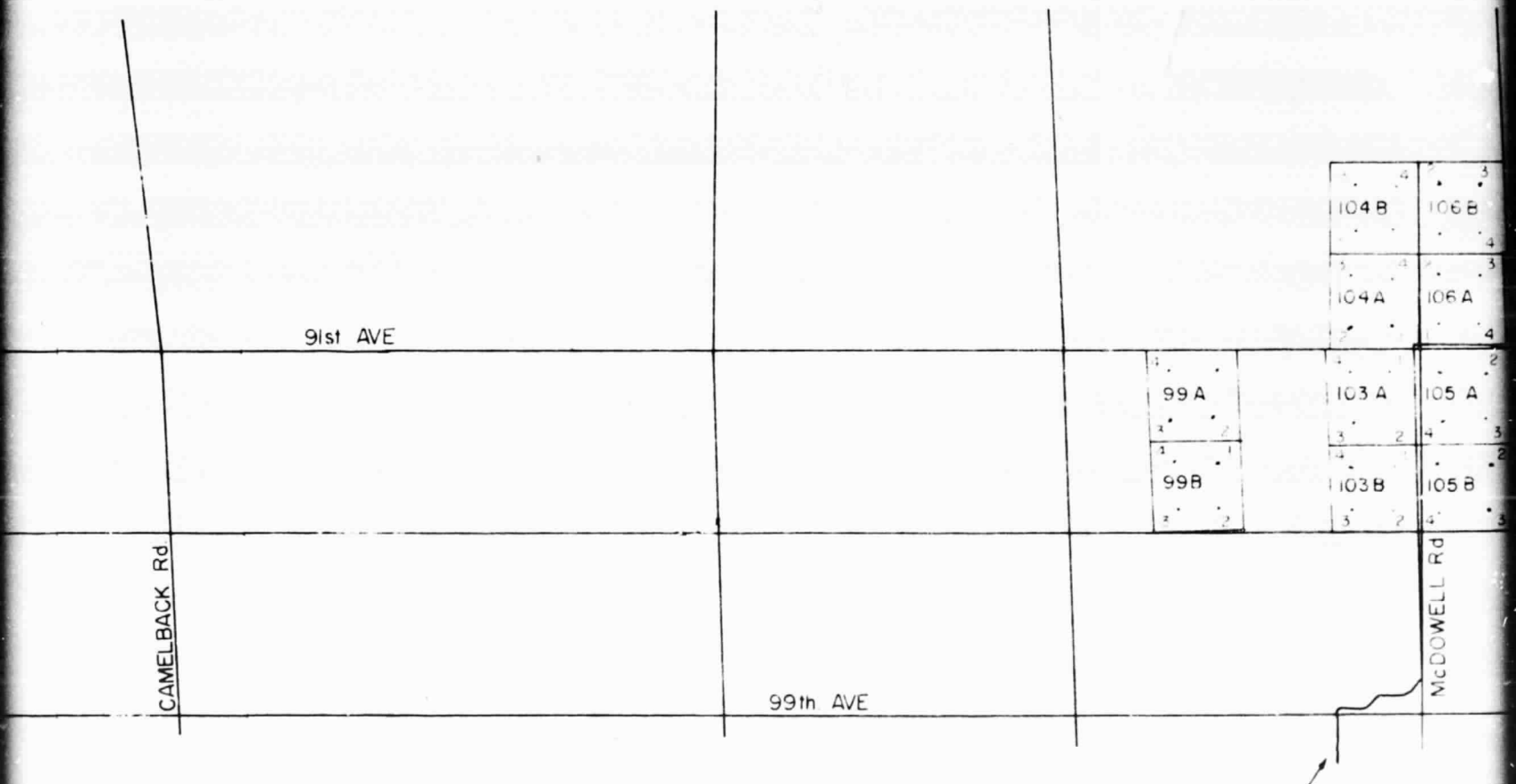

ORIGINAL PAGE 19
OF POOR QUALITY

FOLDOUT FRAME 3

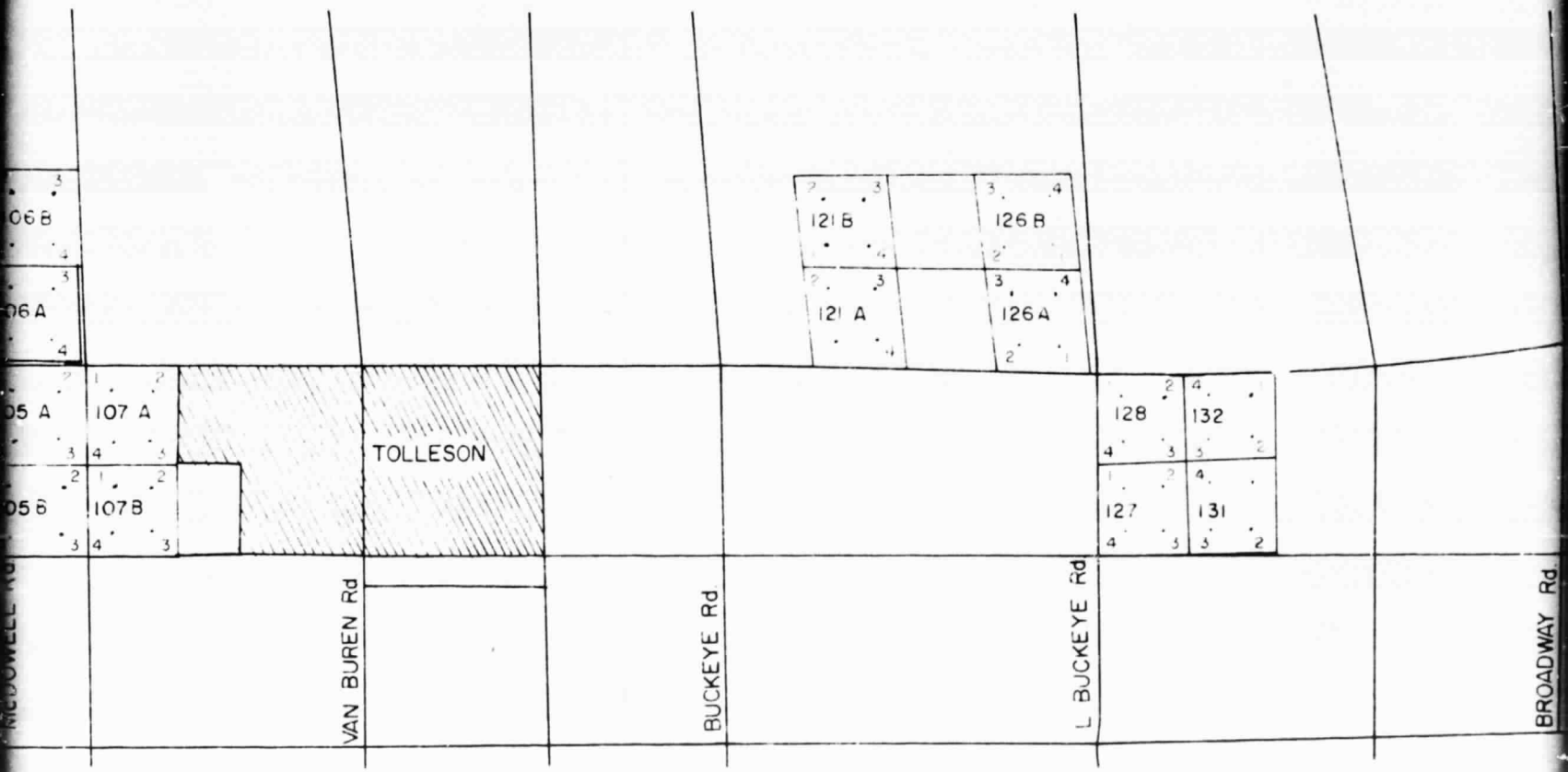

FOLDOUT FRAME

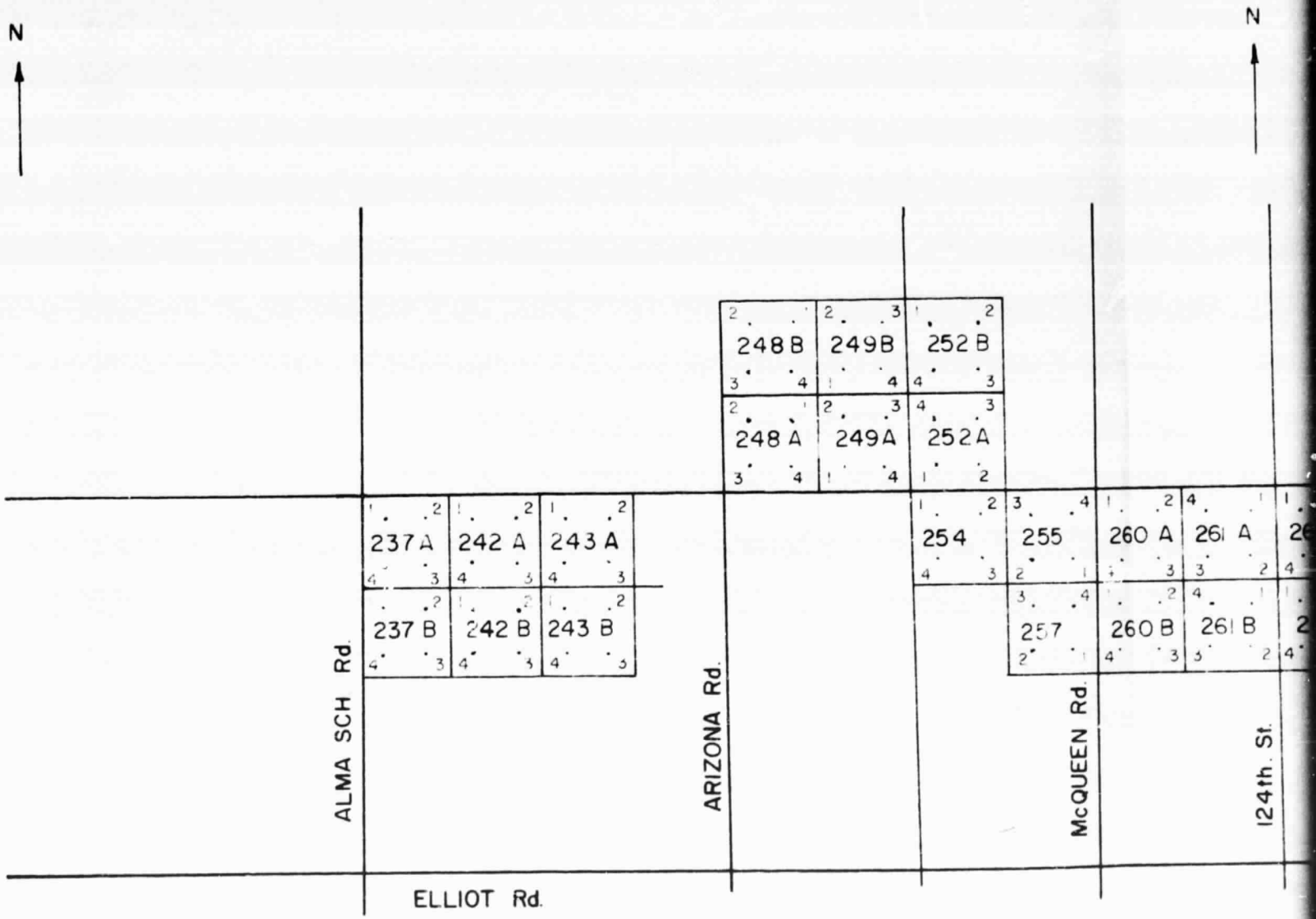

Map 2. E-W Test Site. (From Blanchard, 1974).

ORIGINAL PAGE IS
OF POOR QUALITY

FOLDOUT FRAME

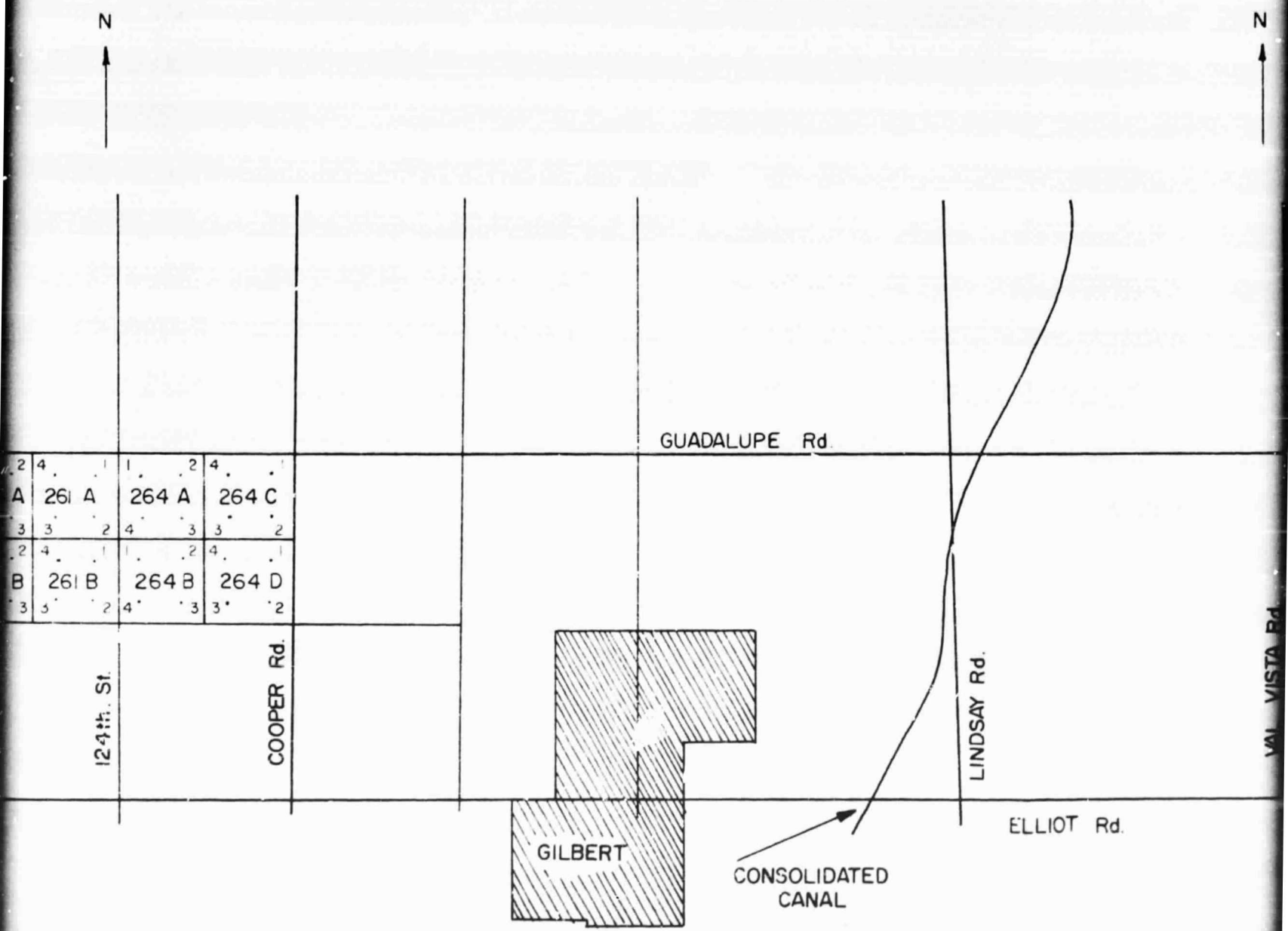

FOLDOUT FRAME 2

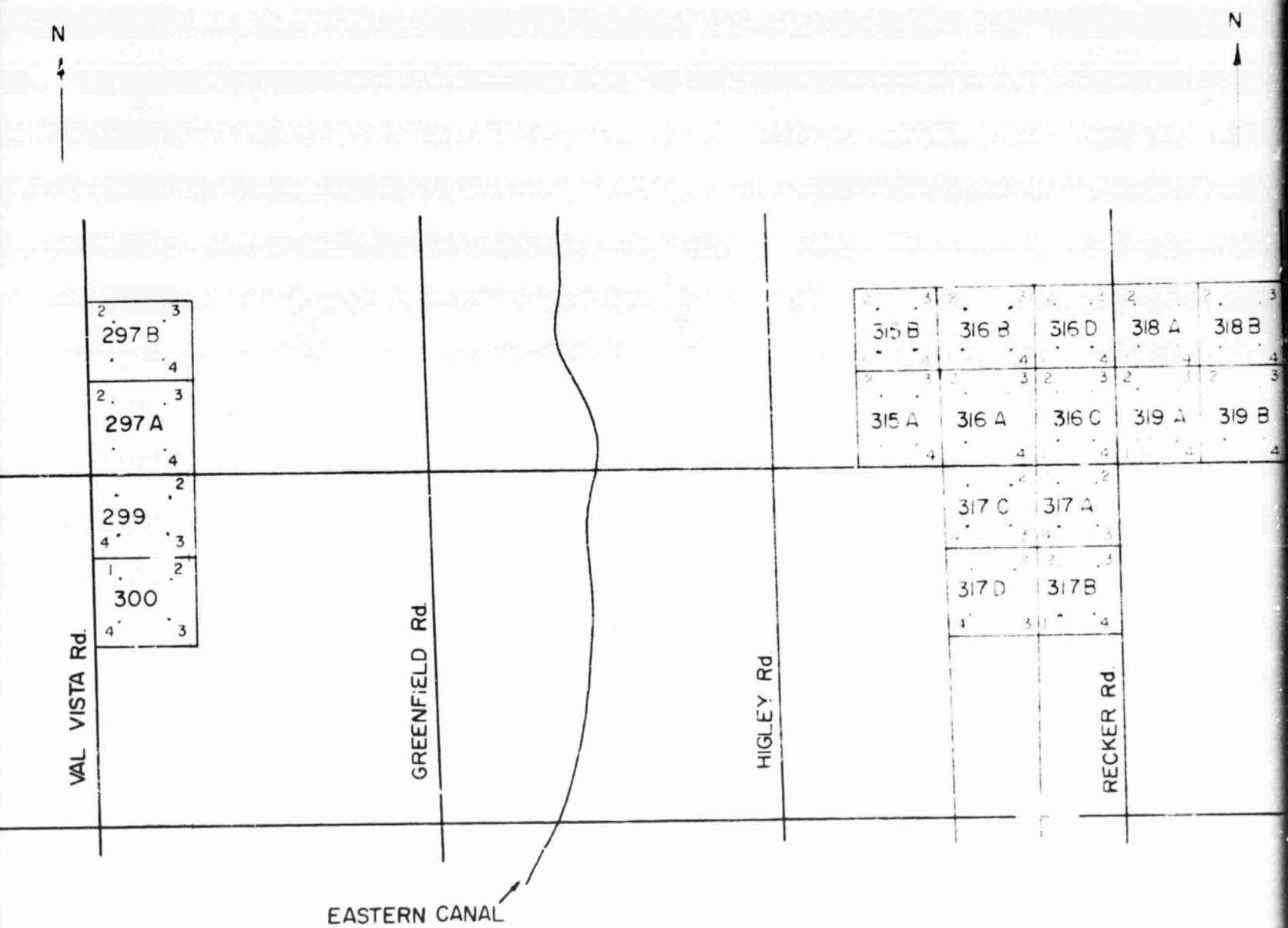

FOLDOUT FRAME 3

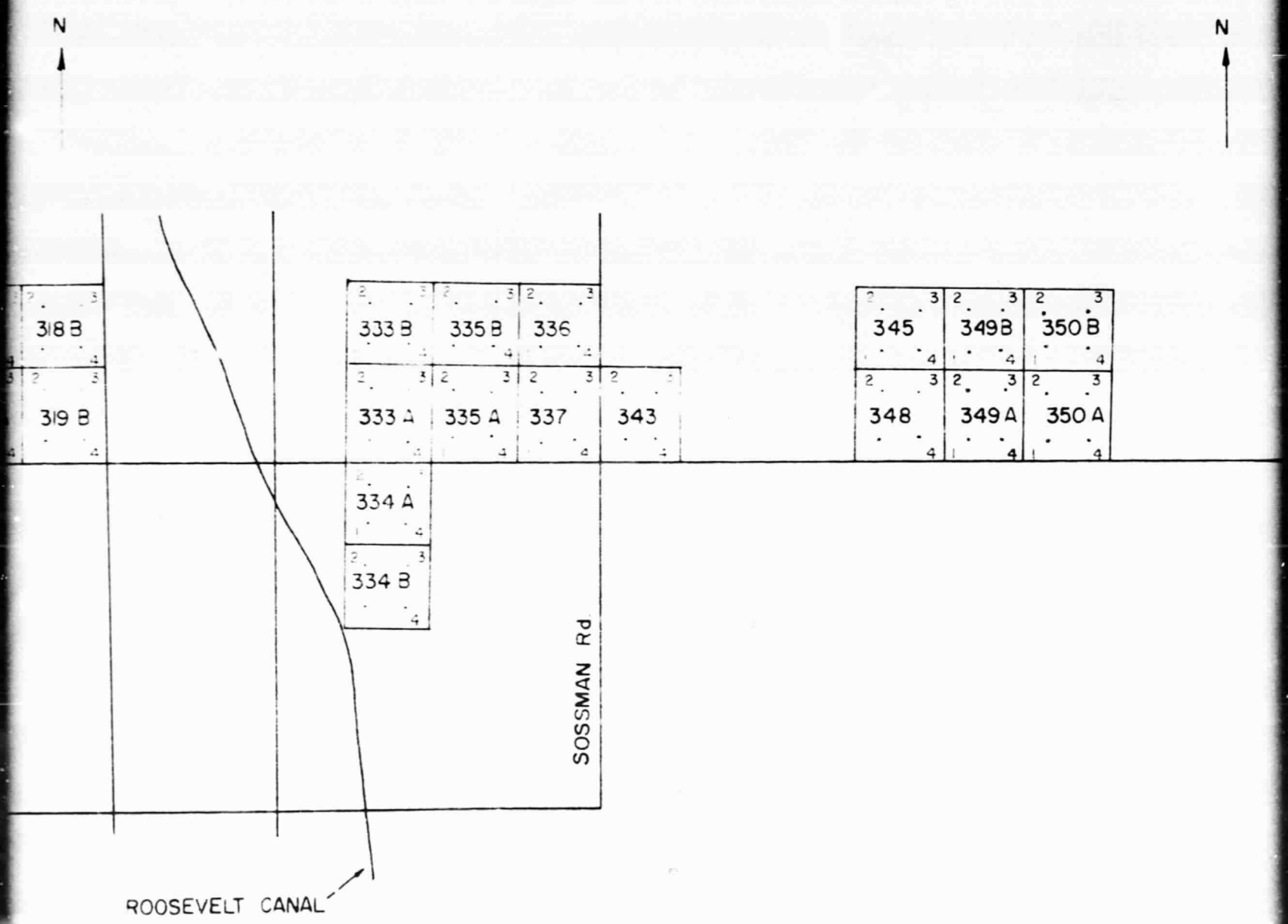

FOLDOUT FRAME 4

3. RADAR SYSTEM

The radar system flown on the April 5, 1974 mission was the Environmental Research Institute of Michigan (ERIM) dual-frequency, dual-polarization synthetic aperture radar. In this system, the along-track resolution is obtained from the synthetic aperture technique, while the cross-track resolution is acquired from FM-pulse compression (Rawson and Smith, 1974). During the flight mission which took place between 1328 and 1630 hrs., the system operated at two frequencies (X-band or 9.375 GHz, and L-band or 1.304 GHz) and two polarization configurations, namely HH (horizontal transmit-horizontal receive) and HV (horizontal transmit-vertical receive). For the NS section, angle of incidence (relative to nadir) ranged between 43° and 57° (in the cross-track direction) and the aircraft's flight path was West of the test site. For the EW section, angle of incidence varied between 27° and 44° at the West end of the section and 23° to 39° at the East end of the section because of an incomplete alignment of the aircraft relative to the test site, and the flight path was North of the site. The radar signals were recorded on signal film during the mission and subsequently processed. The data were provided in the form of radar imagery at an average along/cross-track scale of approximately 1:275,000 (L-band) and 1:600,000 (X-band), separately for each of the frequency/polarization combinations. Also, the ERIM personnel prepared a digital version in which all four frequency/polarization combinations were registered, digitized, and recorded on a magnetic tape. Since the tape data were free of second film recording and processing distortions, they were used exclusively in the data analysis reported herein.

To transform digitized data into a form in which they could be related to ground data, a computer printout of the magnetic tape was generated. Secondly, field boundaries were outlined on the printout using tone changes, the small scale radar imagery, and color infrared aerial photographs taken during the flight mission. Since most fields had a rectangular shape, their extent could then be conveniently specified by identifying rows and columns on the printout. Once data points within each field were determined, mean and standard deviation of the field's radar returns could be computed; all radar returns were expressed in relative units. Since all four frequency/polarization combinations were registered, field boundaries were identified only once. To eliminate possible effects of field boundaries on the

computed statistics, data points within a narrow strip along the field boundary were excluded in the calculation of the mean return and standard deviation.

In the digital imagery supplied by ERIM, the antenna pattern and propagation effects were not incorporated. Instead, curves of the relative radar response as a function of antenna depression angle were calculated for each band and each pass. The following is a description from the ERIM report (1975):

> "The relative radar response for the Phoenix, Arizona, North-South pass is shown in Figure 4*. The response is plotted as a function of ground range, with separate plots given for the X- and L-band channels. In addition, separate curves are given for point-target and extended horizontal target (clutter) scatterers. The difference between the response to these types of scatterers is due to the projection of slant range area onto the ground range plane. The plots shown in Figure 4 cover a ground range of 1/2 mile on either side of 91st street.
>
> Figures 5 and 6 give similar curves for the Phoenix, East-West Pass. In making this pass the aircraft did not fly exactly parallel to Guadalupe Road, causing the slant range to change (decrease) with time. Taking this fact into account the relative response is given for the beginning of the pass and the end of the pass in Figures 5 and 6, respectively. The responses plotted in Figure 5 apply at the start of the E-W data (West end) while those plotted in Figure 6 apply to the end of the E-W data (East end). Between these two points the response should progress linearly with azimuth position from the former to the latter."

The angular response curves shown in Figures 1-3 are calculated from antenna patterns measured in an anechoic chamber in conjunction with slant range calculations based on the aircraft altimeter recording. Prior to applying these curves to the digitized imagery, a section of the imagery was chosen such that the variations in target parameters (moisture content, row direction and vegetation types) were minimal. No discernible pattern of decreasing (or increasing) intensity across the image was observed. Hence it was concluded that if corrections to the digitized return were applied using the calculated angular response curves, the far range fields would have returns as much as 10 times larger than fields in the near range. According to both theory and experimental data (Ulaby et al., 1974), the return is

*Figures 4-6 of the ERIM report are reproduced here as Figures 1-3.

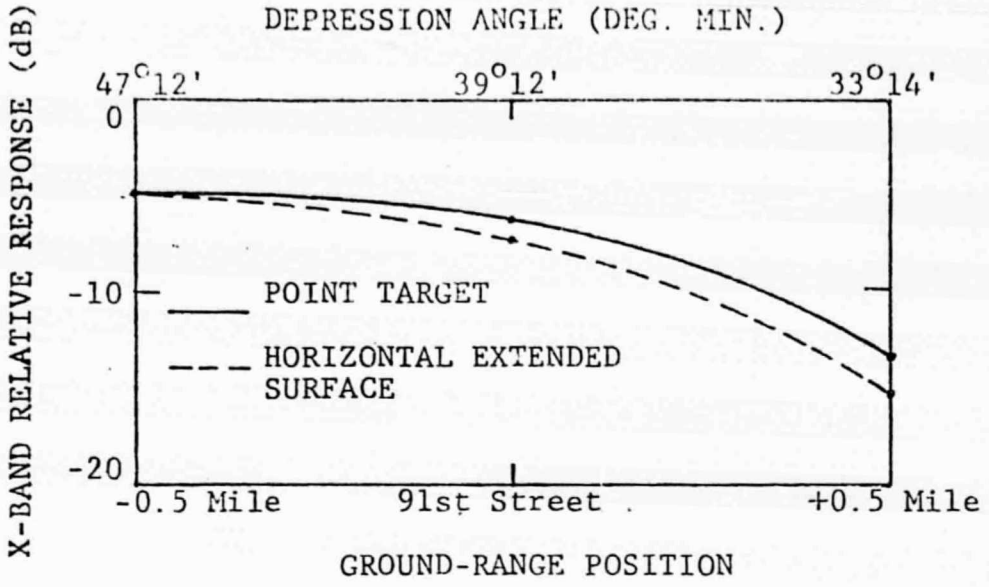

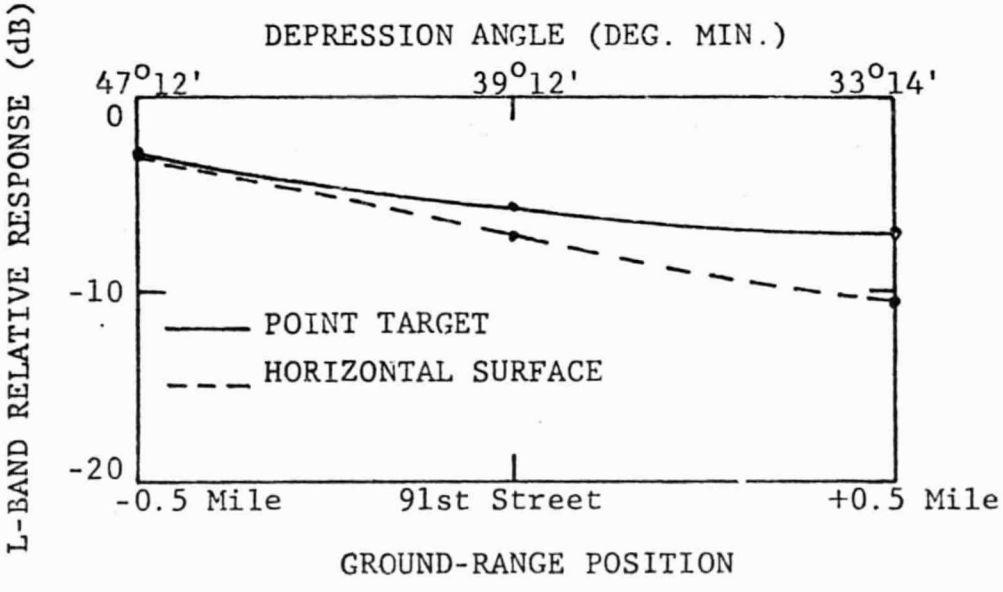

FIGURE 4. RELATIVE RADAR RESPONSE, PHOENIX, ARIZONA, N-S PASS, AREAS A, B, 5 APRIL 1974.

Figure 1. (From ERIM, 1975).

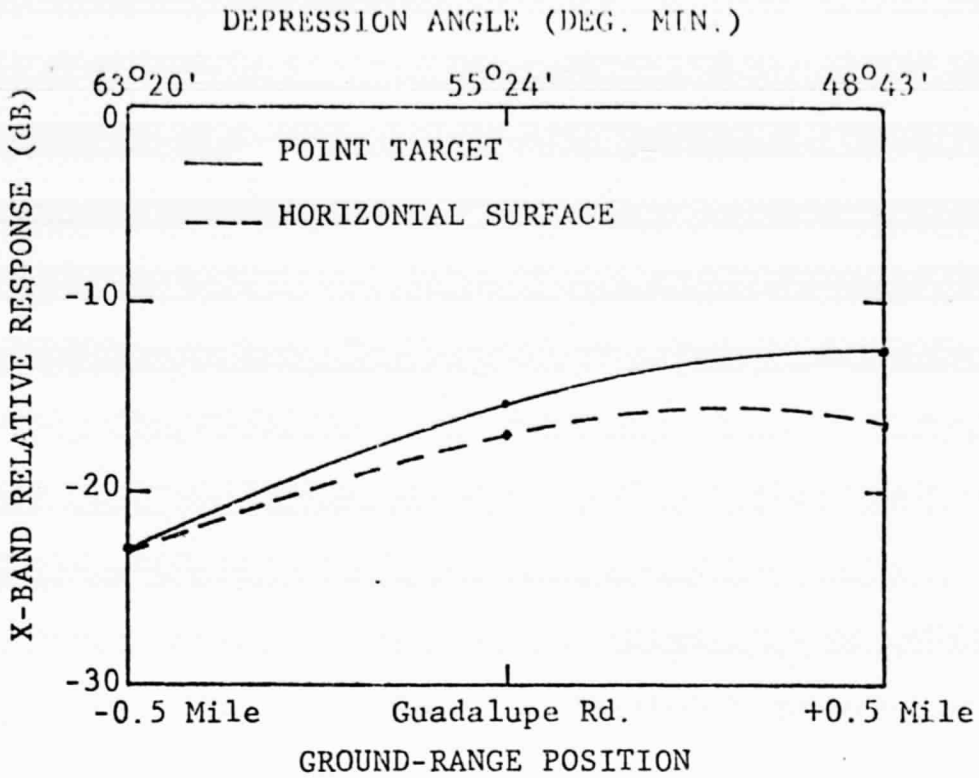

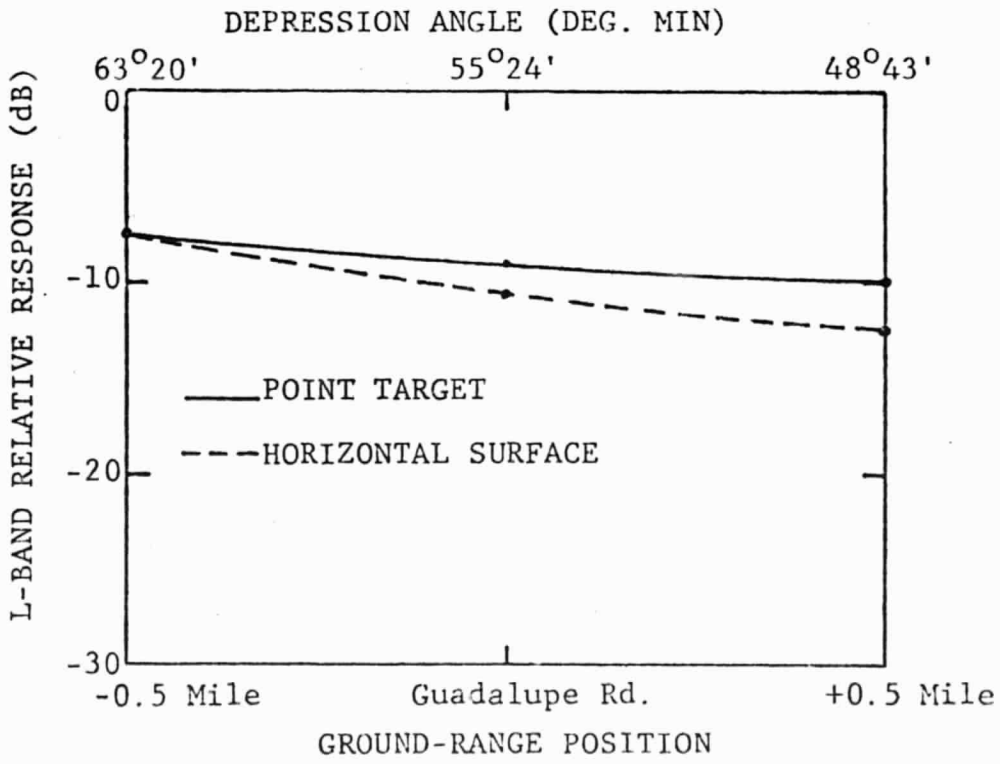

FIGURE 5. RELATIVE RADAR RESPONSE, PHOENIX, ARIZONA, E-W PASS (START OF AREA A), 5 APRIL 1974.

Figure 2. (From ERIM, 1975).

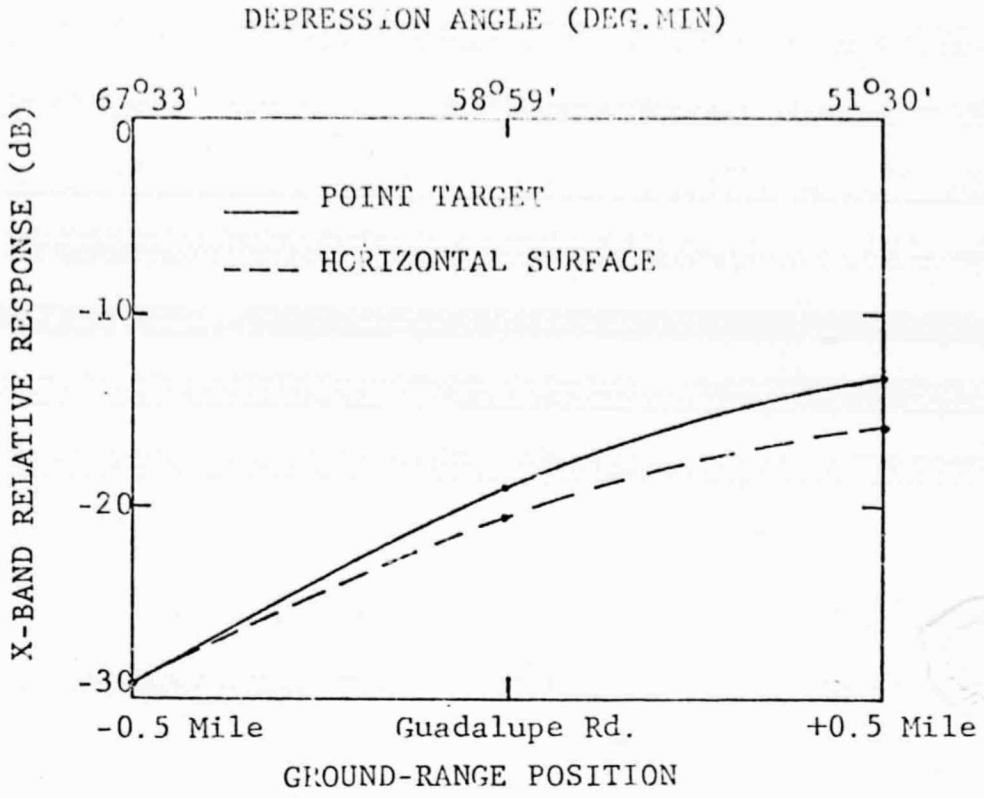

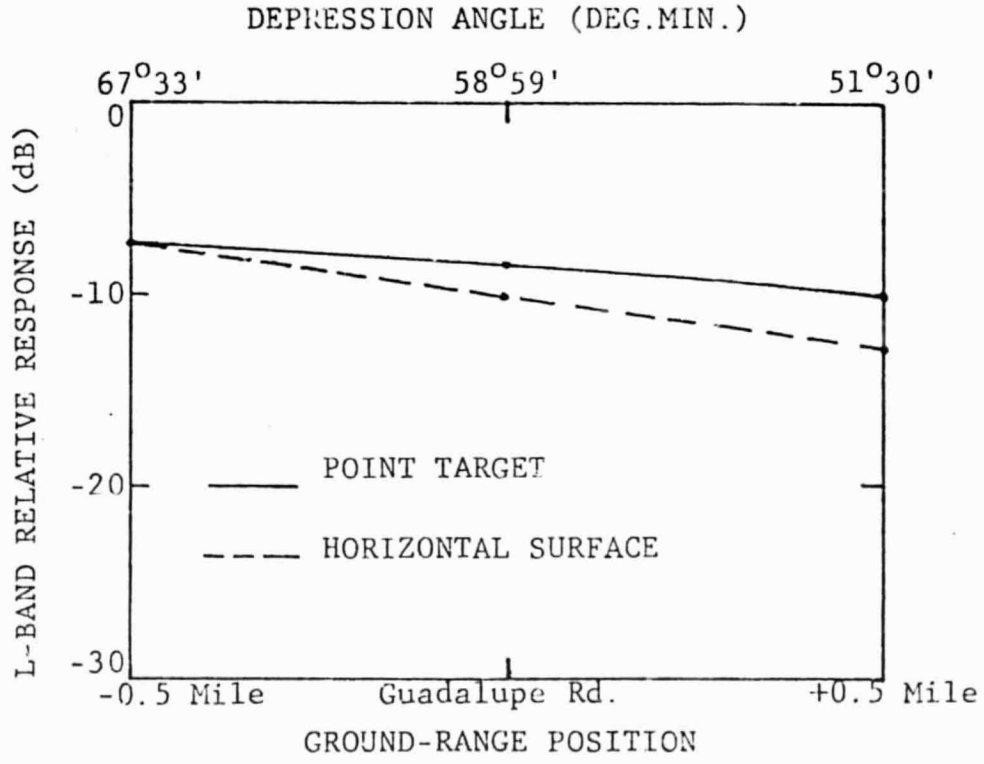

FIGURE 6. RELATIVE RADAR RESPONSE, PHOENIX, ARIZONA, E-W PASS (END OF AREA 6), 5 APRIL 1974

Figure 3. (From ERIM, 1975).

expected to decrease, not increase, with increasing angle of incidence (relative to nadir). Consequently, it was decided that data presented in Figures 1-3 could not be used to correct the measured radar returns. It should be noted that ERIM personnel independently reached the same conclusion*.

4. SURFACE MEASUREMENTS

The bulk of ground data was collected from bare fields in the following way:

(i) Prior to the flight mission, surface roughness measurements were made using a thin aluminum plate. The plate was inserted vertically into the ground and the surface roughness contour was photographed against the plate as a background. Figure 4 shows an example of such roughness profile. Since most bare fields were prepared for cotton and therefore had roughnesses which differed in two perpendicular directions, three roughness profiles were taken: two parallel to rows (one on top of the ridge (Figure 4a), one at the bottom) and one across the rows (Figure 4b).

(ii) Between 1000 and 1630 hours on 5/4/74, soil samples were taken for soil moisture content determination of bare fields. As a rule, four sites were sampled per field, each site being approximately 50 m diagonally distant from the field's corner. For dry fields, only ridge tops were sampled, while both tops and bottoms were sampled when moisture content in the top 5 cm of the soil was medium or high. In either case, five soil samples were taken per profile from the following depths (relative to the local soil surface): 0-1 cm, 1-2 cm, 2-5 cm, 5-9 cm, and 9-15 cm. Samples were placed into plastic bags, and gravimetric water content was determined after drying the soil. Resulting soil water content values in percent by dry weight for 86 fields were reported by Blanchard (1974).

*Dr. Dale Ausherman, Radar Optics Laboratory, Environmental Research Institute of Michigan, Ann Arbor, Michigan, personal communication.

Figure 4a. Photograph of field 318 with plate inserted parallel to the rows.

ORIGINAL PAGE IS
OF POOR QUALITY

Figure 4b. Photograph of field 275 showing the plate inserted perpendicular to the row direction.

ORIGINAL PAGE IS
OF POOR QUALITY

(iii) A limited number of soil samples were taken for bulk density estimation. Bulk density was considered a necessary parameter since for most practical purposes, the amount of water present must be stated in volumetric units, and soil water content can be specified volumetrically only if bulk density is available. Figure 5 gives the results for the ridge top and bottom, respectively.

Prior to analyzing the relationship between the radar return and soil moisture, moisture profiles reported by Blanchard (1974) were processed in the following manner. First, the gravimetric water contents were converted into volumetric water content using the bulk density profiles (Figure 5). Secondly, mean soil moisture profiles were computed for sites in which both top and bottom positions were sampled by averaging moisture values for equivalent depth intervals. Thirdly, the mean moisture profiles (or profiles of ridge tops for dry fields) were multiplied by "soil moisture correction coefficients" empirically evaluated for dry and wet fields by Blanchard (1974). These corrections were computed so as to account for the varying soil moisture distribution between ridge tops and bottoms on the bare fields. Since the coefficients for the various angle of incidence ranges and look directions were similar at equivalent depth (Blanchard, 1974,p. 17), only one set of correction coefficients was used for dry fields, and one set for wet fields. Based on personal communication with B. J. Blanchard*, a field was considered wet if the mean moisture content for the 9-15 cm depth was above 0.24 cm^3/cm^3 (20% of dry weight). Fourthly, moisture values were interpolated between the five values measured and extrapolated to a 15 cm depth so that soil moistures in cm^3/cm^3 were available for 1 cm increments between 0 and 15 cm depth. These profiles were used in the final step to calculate m, the effective moisture content within a half-skin depth, where half-skin depth was defined as the depth at which the cumulative attenuation reached 0.5 (Batlivala and Cihlar, 1975). The values of half-skin depths were computed using the procedure described by Ulaby et al. (1974), and dielectric constant data reported by Cihlar and Ulaby (1974).

---

* Dr. B. J. Blanchard, Texas A&M University, College Station, Texas.

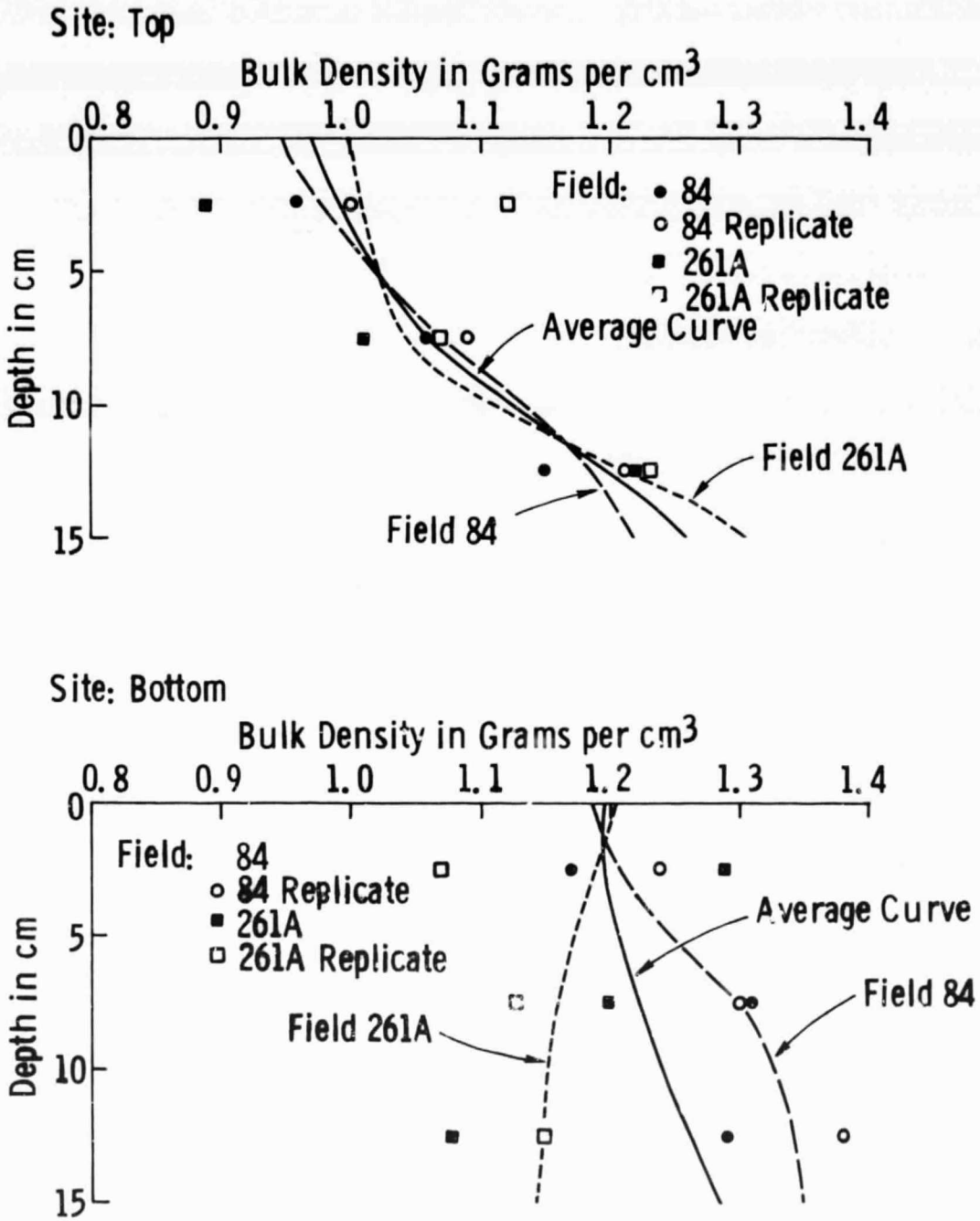

Figure 5. Bulk density profiles based on samples from several depths at each of two locations: Top of the furrow, and bottom of the furrow.

5. RESULTS AND DISCUSSION

Radar return values acquired by the above described procedure were subjected to extensive analyses. The objective of these analyses was to identify those ground parameters to which the radar responded and, in particular, the relationship between radar return and soil moisture content. Both measured and derived variables were used in this procedure.

Figures 6 through 9 are examples of the originally provided small scale radar imagery for the four channels (i.e., frequency/polarization combinations) and both flight line sections (passes). A brief examination of the images suggests that consistent differences in gray tone levels between the two flight line sections occurred, particularly in the X-band (Figures 6 and 7). To verify this observation, radar return values computed for individual fields were plotted in Figures 10 and 11; both bare and vegetated fields were represented.

In the case of X-band, HV values were approximately equal to HH values for the NS pass but much smaller for the EW pass. Since ground conditions were similar for both passes (e.g., average moisture content in the 0-1 cm layer was 0.024 cm^3/cm^3 and 0.023 cm^3/cm^3 for the NS and EW sections, respectively), the systematic shift in radar return values appears to be due to the sensor response. The actual cause of the changing response was not identified but could be attributed to different degrees of depolarization over the two angular ranges (corresponding to the two passes). According to ERIM personnel*, the sensor settings were not readjusted between the two flight passes. Because X-band radar return values measured on the NS pass fall within a very narrow range (Figure 10) and due to low moisture contents in the near-surface soil layers for most bare fields, the X-band responses to soil moisture could not be studied effectively.

A similar situation was encountered in the case of L-band although the differences between polarizations were smaller here. Figure 11 indicates that the L-band HH return R_L(HH) was greater than R_L(HV) for the NS pass but both were of nearly equal magnitude for the EW pass. Consequently, to allow for this differential, it was decided to analyze the NS and EW L-band measurements separately.

*Dr. Dale Ausherman, personal communication.

ORIGINAL PAGE IS
OF POOR QUALITY

Far Range

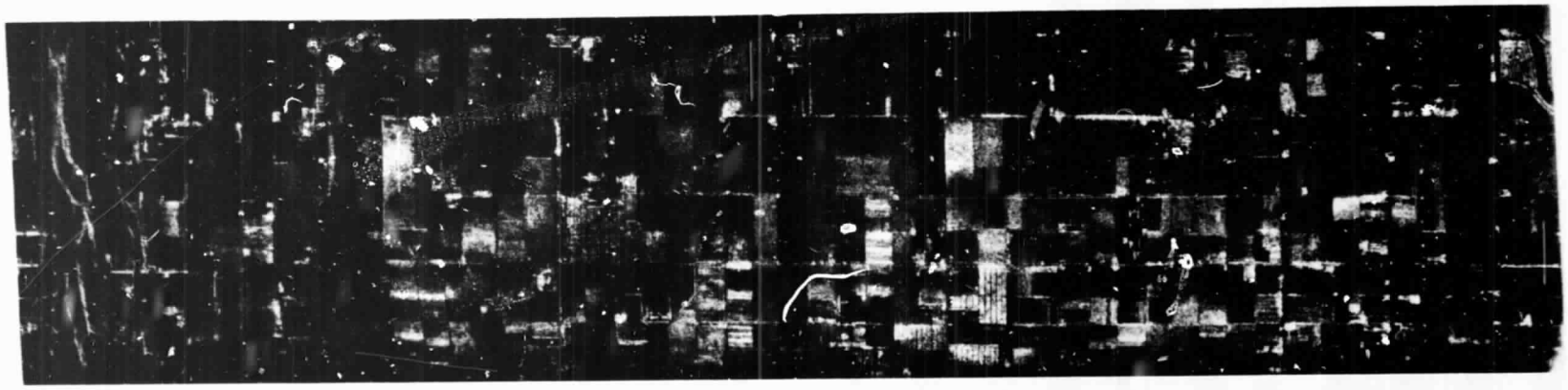

Near Range

(a) HH polarization

N →

Far Range

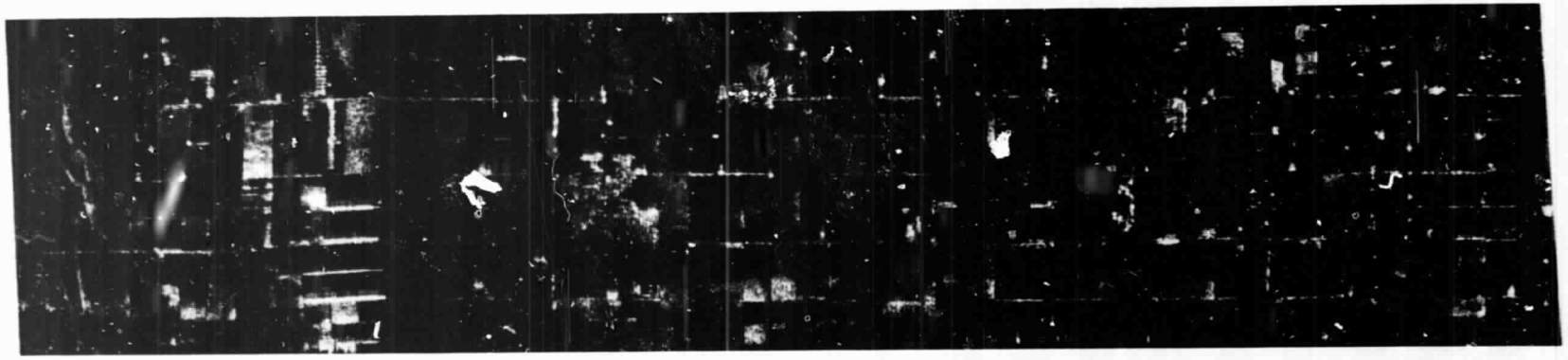

Near Range

(b) HV polarization

Figure 6. L-band imagery of a portion of the NS pass. a) HH polarization and b) HV polarization. (Courtesy of ERIM).

Far Range

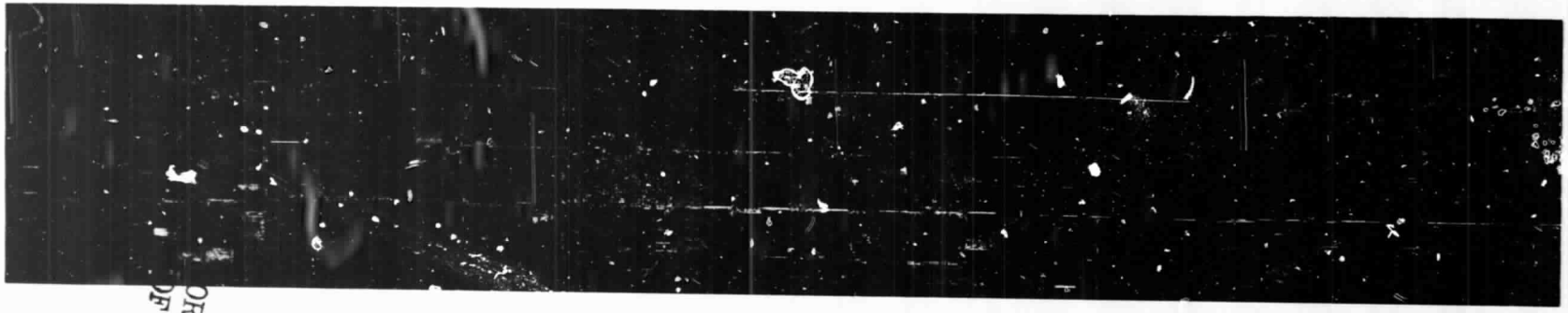

ORIGINAL PAGE IS
OF POOR QUALITY

Near Range

(a) HHpolarization

N →

Far Range

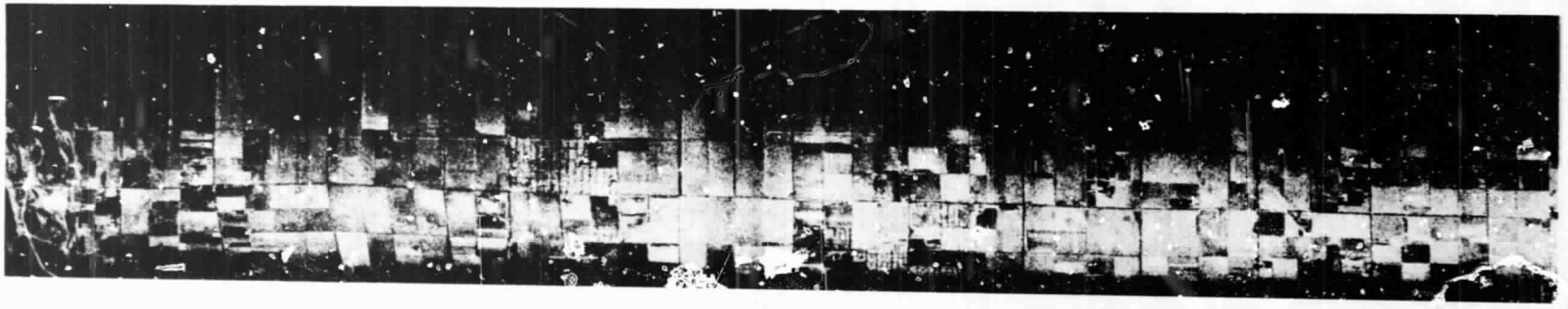

Near Range

(b) HV polarization

Figure 7. X-band imagery of a portion of the NS pass. a) HH polarization and b) HV polarization. (Courtesy of ERIM).

Far Range

Near Range

(a) HH Polarization

N →

Far Range

Near Range

(b) HV Polarization

Figure 8. L-band imagery of a portion of the EW pass. a) HH polarization and b) HV polarization. (Courtesy of ERIM).

Far Range

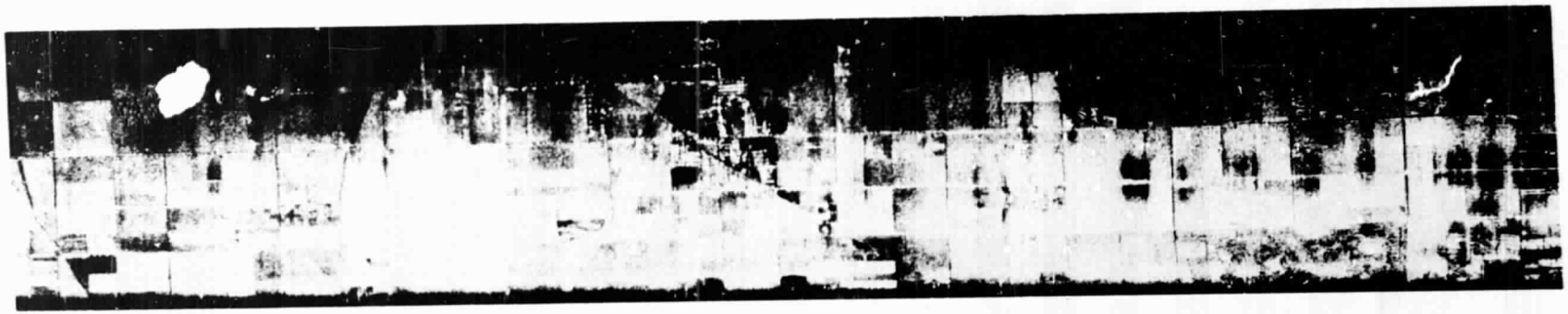

Near Range

(a) HH polarization

N →

Far Range

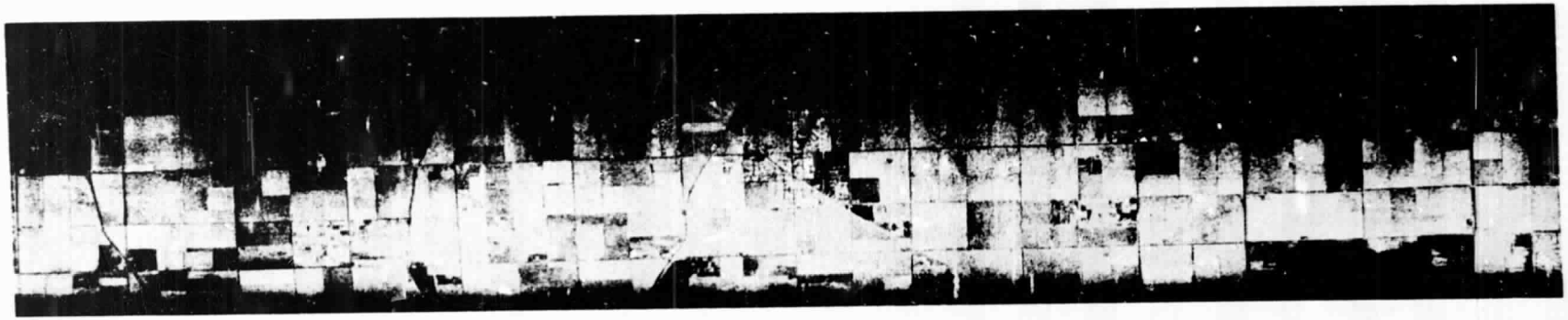

Near Range

(b) HV polarization

Figure 9. X-band imagery of a portion of the EW pass. a) HH polarization and b) HV polarization. (Courtesy of ERIM).

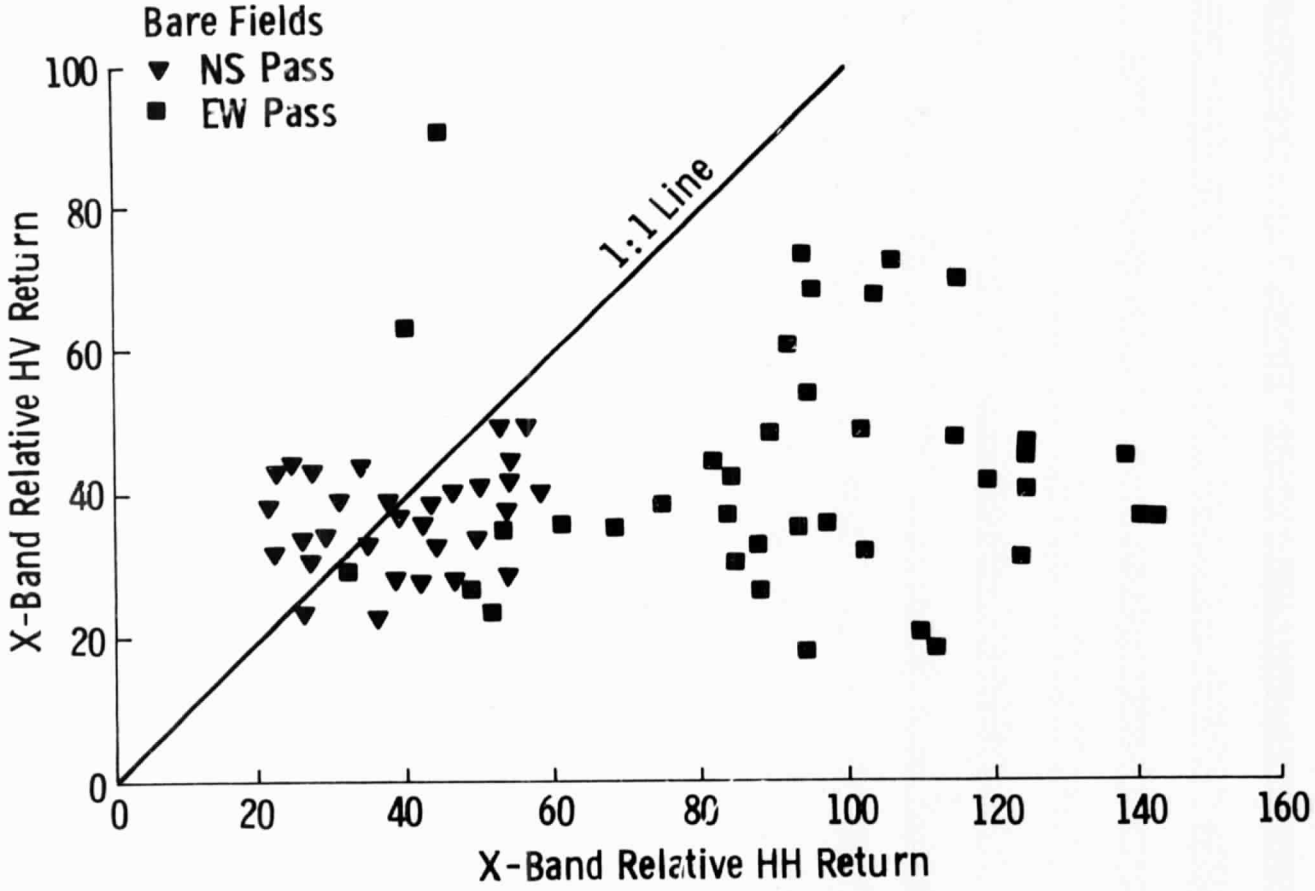

Figure 10. Scattergram comparing the X-band depolarization of the NS pass with the EW pass.

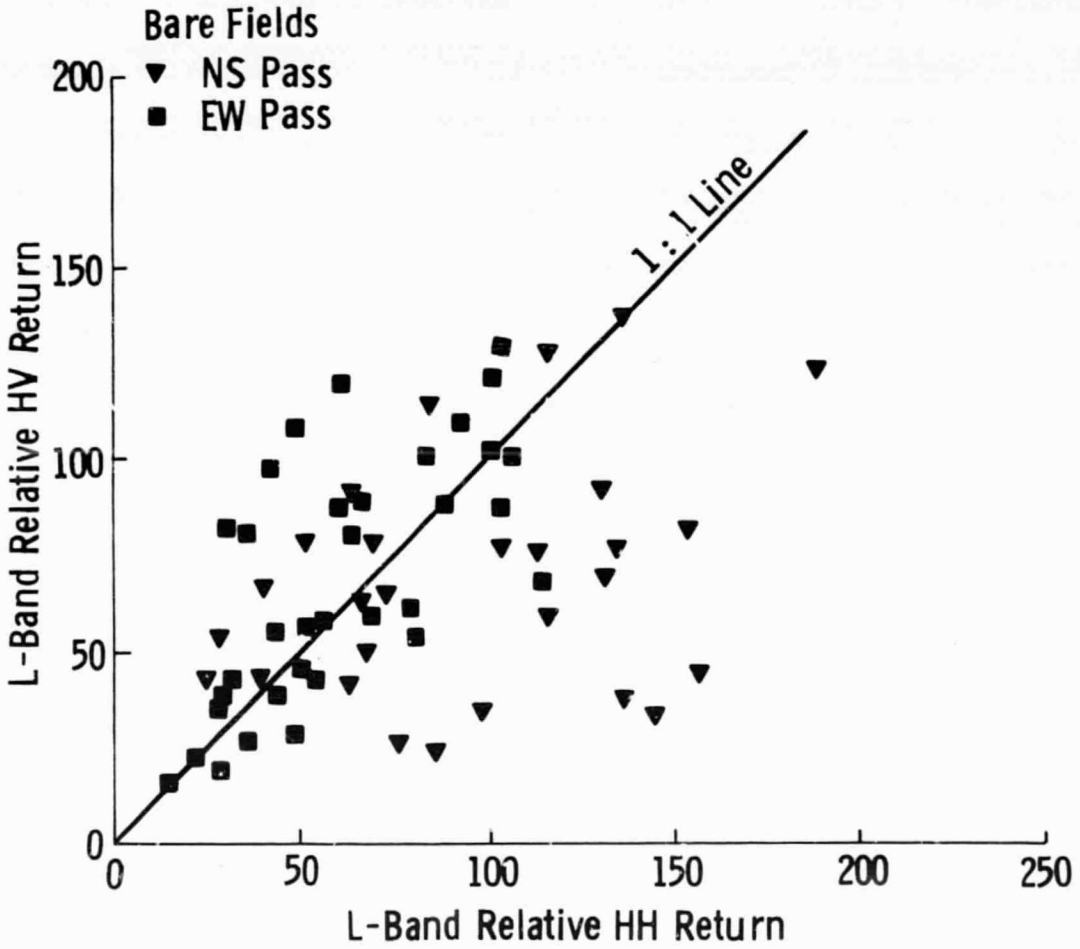

Figure 11. Scattergram comparing the L-band depolarization of the NS pass with the EW pass.

Since radar returns used to analyze the effect of soil moisture on the microwave signal were not (and could not be) corrected for the cross-track antenna pattern variations, they would be expected to show only a limited response to soil moisture. This was indeed the case as is evident from the following discussion.

5.1 Response to Moisture Content

Figures 12 and 13 show R_L(HH) and R_L(HV) values plotted against the effective soil moisture content within the half-skin depth for NS and EW bare fields, respectively. Based on theoretical considerations as well as experimental measurements (Ulaby et al., 1974), the radar return should increase with moisture content. Such a trend is not apparent in Figures 12 and 13, however. Similarly, no discernible patterns could be extracted when R_L(HH) or R_L(HV) were plotted against soil moisture content in the 0-1 cm, 0-2 cm, 0-5 cm, 0-9 cm or 0-15 cm.

In the absence of a reliable response pattern that can be used to correct for the variations across the image due to antenna gain and range differences, the decision was made to divide the one-mile cross track dimension of the test site into four separate ranges, each extending 0.25 miles. Although this division resulted in non-equal angle-of-incidence ranges, it was convenient as far as the analysis was concerned because the majority of the fields were either 0.25 miles or 0.5 miles wide. Hence, in a given range, all fields included in the analysis would be 0.25 miles wide. Thus, antenna gain and range effects would have approximately the same influence on the return from each of these fields.

For the NS pass, the aircraft height was 9000 feet and the angle of incidence varied between 43° and 57° in the cross track direction (1 mile wide). R_L(HH) and R_L(HV) of fields in ranges 1 through 4 are shown in Figures 14 and 15. It is noted that in ranges 1 and 2 both R_L(HH) and R_L(HV) indicate good correlation with soil moisture, whereas in ranges 3 and 4 the radar return and soil moisture appear independent of one another. Due to the limited number of fields in ranges 1 and 2 and due to the narrow range of moisture content covered by these fields, caution should be exercised in terms of the conclusions derived from the observed radar response to soil moisture. One wonders, for example, as to why a change of 3° (from ranges 2 to 3) can cause complete loss of sensitivity to soil moisture!

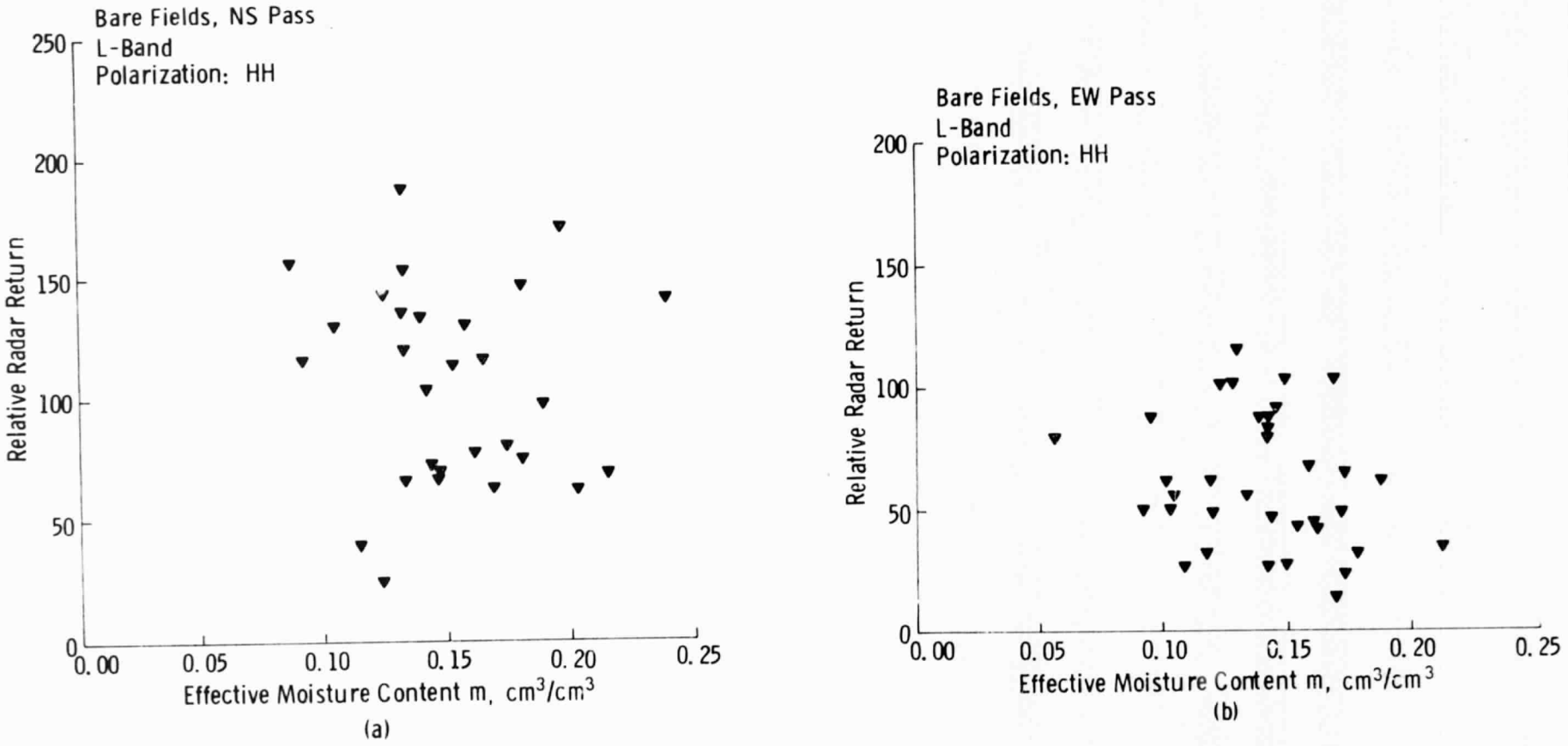

Figure 12. L-band relative HH return as a function of effective moisture content.
a) NS pass, b) EW pass.

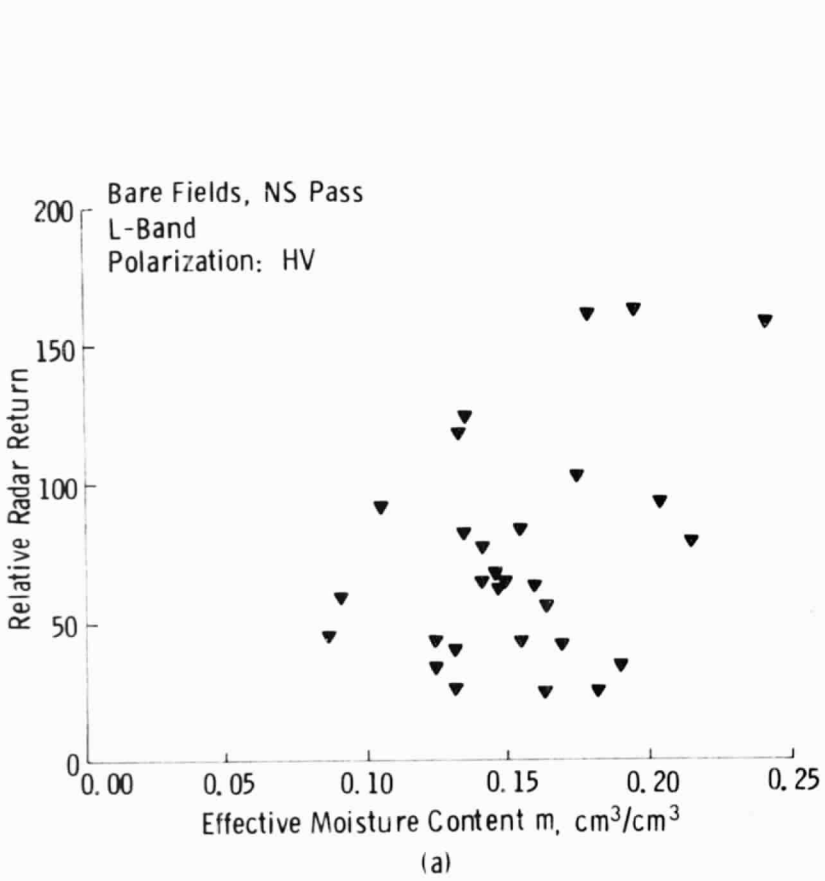

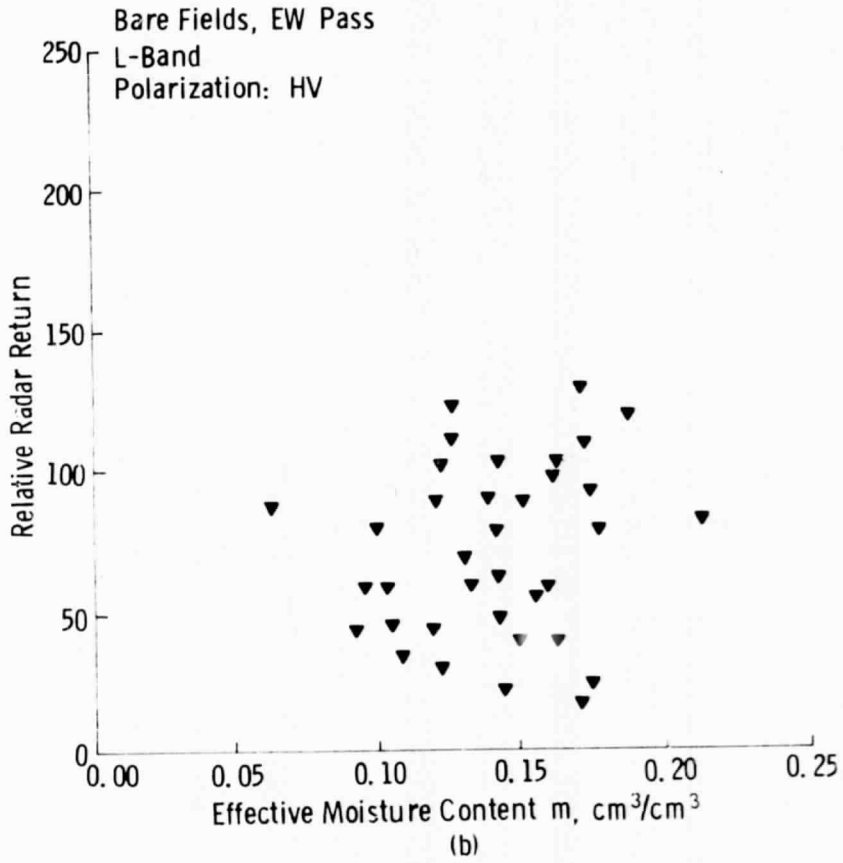

Figure 13. L-band relative HV return as a function of effective moisture content.
a) NS pass, b) EW pass.

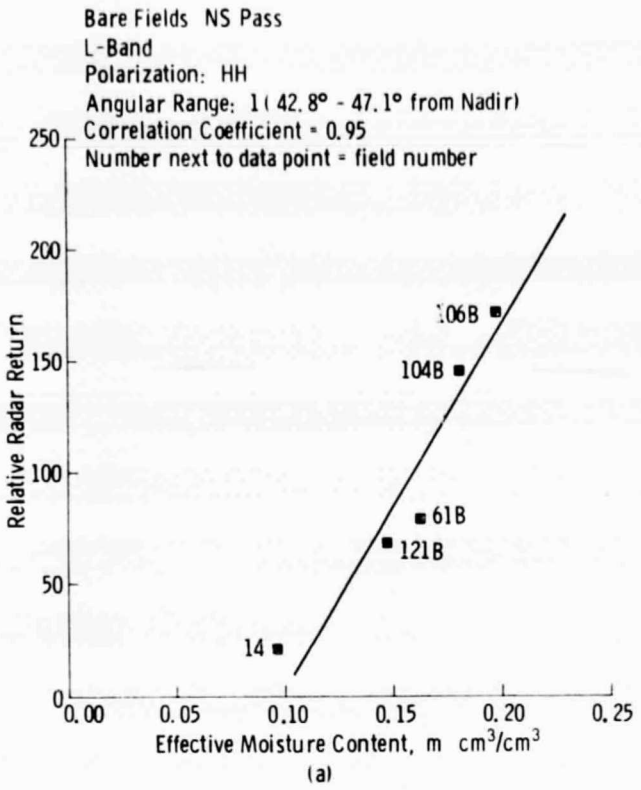

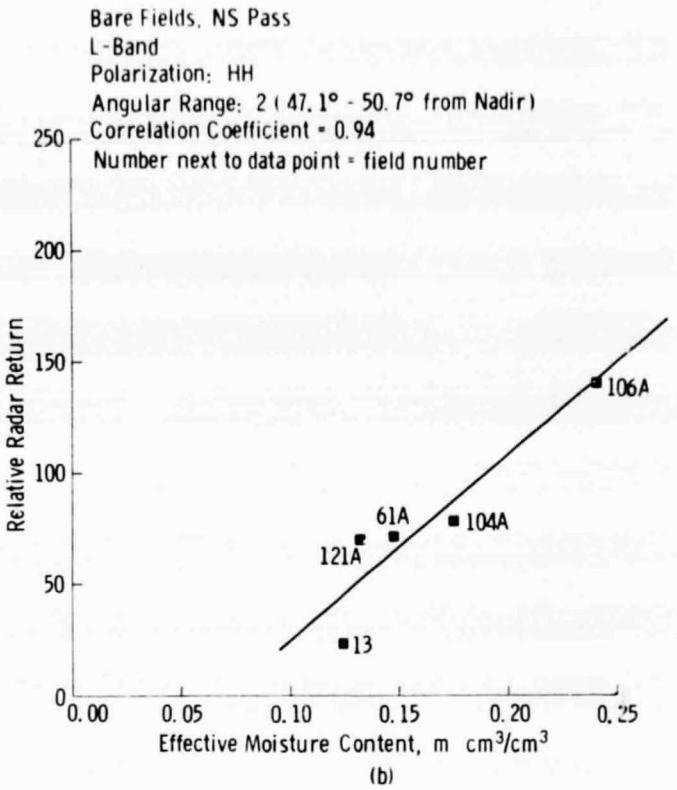

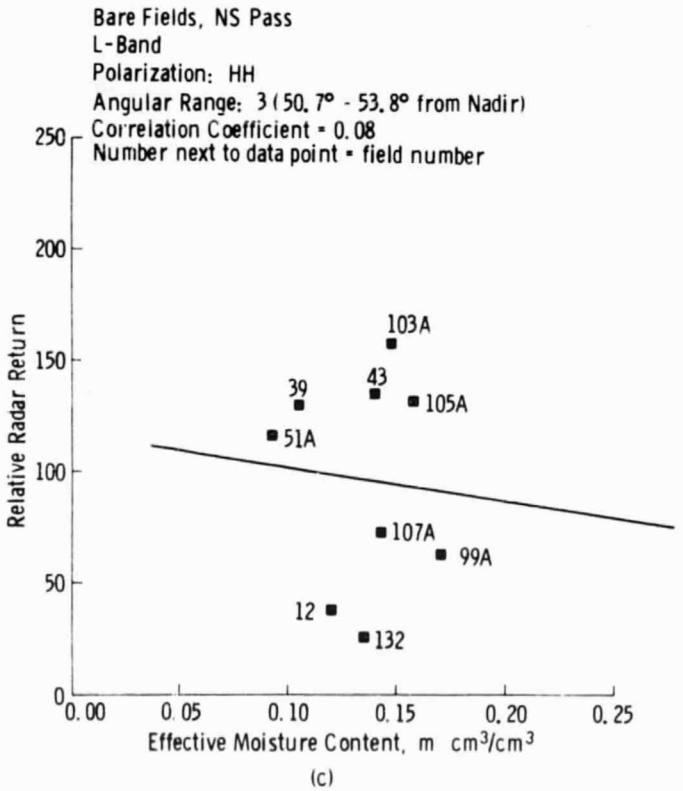

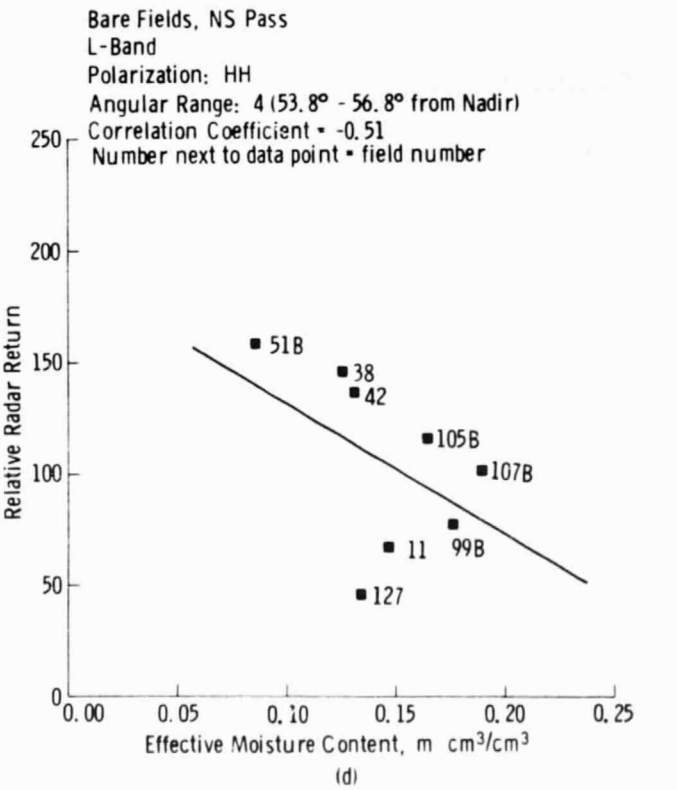

Figure 14. L-band relative HH return as a function of effective moisture content for bare fields in angular ranges: a) 42.8°-47.1°, b) 47.1°-50.7°, c) 50.7°-53.8°, and d) 53.8°-56.8°.

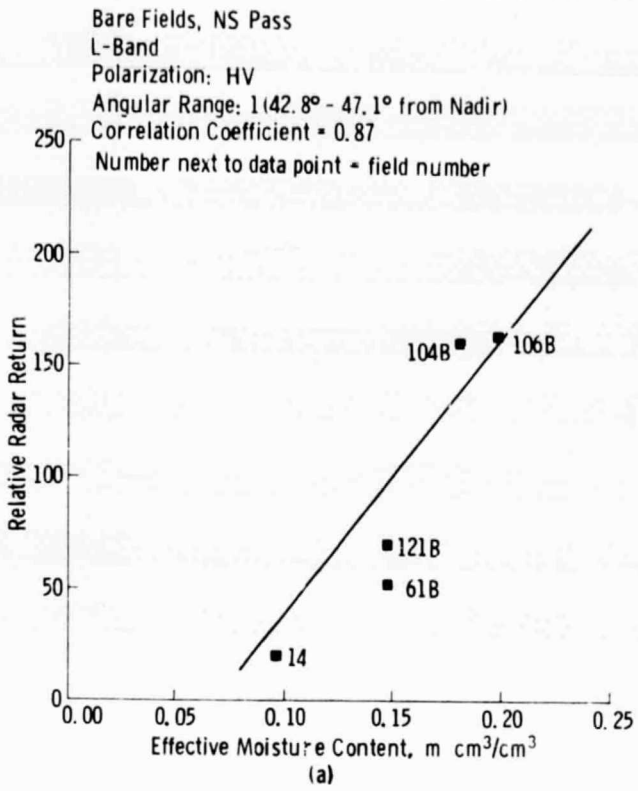

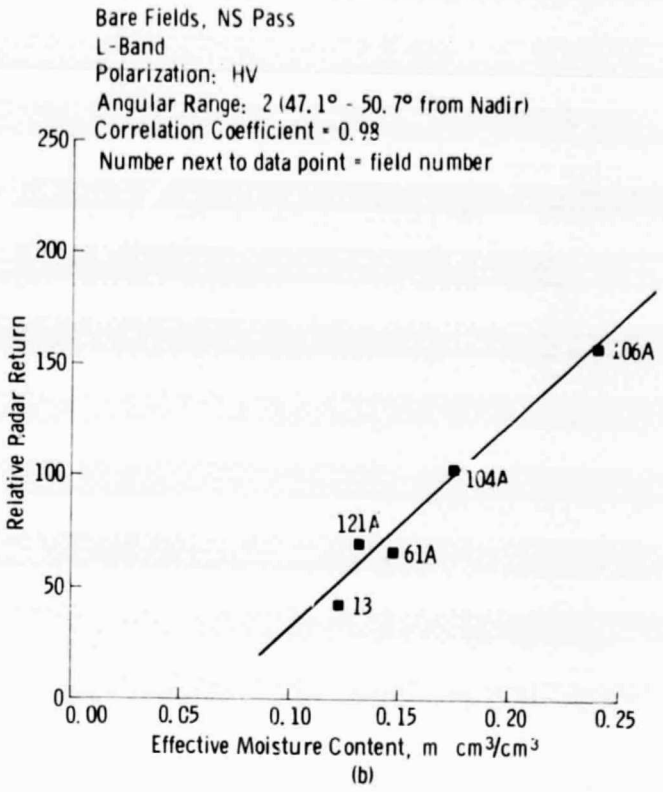

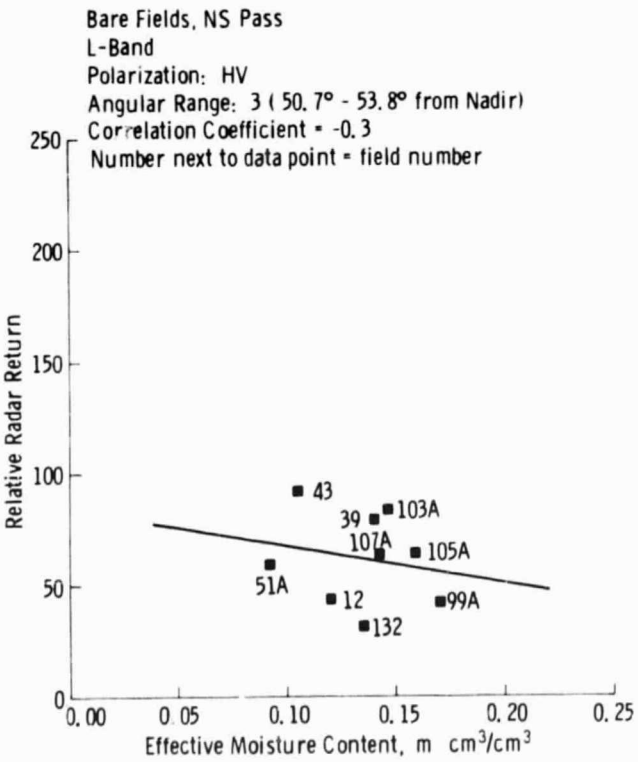

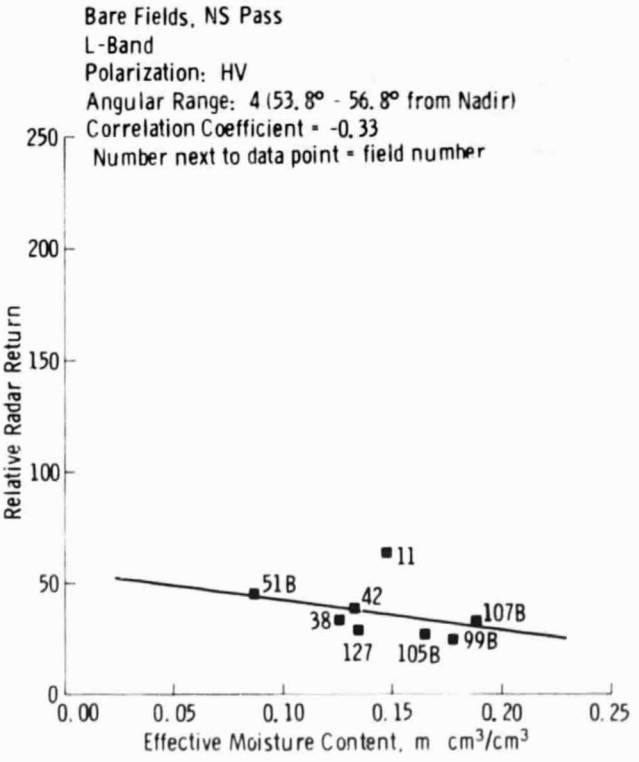

Figure 15. L-band relative HV return as a function of effective moisture content for bare fields in angular ranges: a) 42.8°-47.1°, b) 47.1°-50.7°, c) 50.7°-53.8°, and d) 53.8°-56.8°.

Correlations similar to those described above were also calculated between R_L(HH) and moisture content in the 0-1 cm, 0-2 cm, 0-5 cm and 0-9 cm. The results are summarized in Table 1 .

For the EW pass, the aircraft altitude was 14,000 feet. Due to misalignment with the center line of the test site (Guadalupe Road), the angle of incidence range corresponding to the test site 1 mile width changed from 27°-44° at the West end to 23°-39° at the East end. With the angle of incidence changing, the range to the target also changes. Hence, it was not possible to apply the range division employed for the NS pass.

5.2 Effects of Surface Roughness

An attempt was made to investigate the effect of surface roughness on the measured radar return. Three parameters related to surface roughness were included in this analysis: row direction (relative to the aircraft flight direction), macro-roughness and micro-roughness. The objective was to determine if any one of these parameters was acting as a bias in terms of the radar response to soil moisture.

Apart from the above described antenna pattern and propagation effects, Figures 12 and 13 can be explained by an interferring influence of other variables, both sensor and ground, which either decreased or overrode radar sensitivity to soil moisture. Consequently, an attempt was made to identify the important interferring parameters. Besides soil moisture contents at 5 depth intervals, information on surface roughness (both macro- and micro-) and incidence angle were available.

Since most bare fields were prepared for cotton planting, their surface configurations consisted of parallel ridges oriented in either along-track or cross-track directions. The peak-to-trough distance for these ridges ranged from less than 7.5 cm to 30 cm. Figure 16 shows R_L(HH) for the NS section against m, with the two row directions marked by different symbols. It is apparent that most cross-track fields yielded low radar return but the relation was not consistent. That is, some along-track fields also had low return, and a few cross-track fields yielded high R_L(HH) values. Thus a consistent relationship between radar return and soil moisture was not apparent here even if each of the row directions was considered separately. Similar results were obtained with R_L(HV).

To further explore the effect of row configuration, the peak-to-trough distance range for the ridges was divided into four categories (0-7.5 cm, 7.5-15.0 cm, 15.0-22.5 cm, 22.5-30 cm) and individual fields from the NS section were allocated to

Table 1: Slopes (s) and linear correlation coefficients (r) between the measured relative radar return and moisture content for each of four angle of incidence ranges and five definitions of moisture content.

HH Polarization

	Angular Range 1		Angular Range 2		Angular Range 3		Angular Range 4	
	s	r	s	r	s	r	s	r
m_1	3528	0.84	600	0.63	-4335	-0.39	-1112	-0.20
m_3	1701	0.96	621	0.21	-1163	-0.33	-578	-0.35
m_5	1361	0.96	695	0.87	30	-0.01	-474	-0.40
m_9	1214	0.95	475	0.76	-155	-0.09	-465	-0.47
m	1544	0.95	824	0.94	-143	-.077	-631	-0.51

HV Polarization

	Angular Range 1		Angular Range 2		Angular Range 3		Angular Range 4	
	s	r	s	r	s	r	s	r
m_1	3282	0.73	735	0.73	-1212	-0.25	268	0.15
m_3	1664	0.89	741	0.86	-558	-0.37	-150	-0.29
m_5	1325	0.88	805	0.94	-98	-0.11	-124	-0.33
m_9	1174	0.87	459	0.69	-146	-0.20	-94	-0.30
m	1510	0.87	916	0.98	-169	-0.21	-129	-0.33

Notation:

Angular ranges: 1 = 42.8°-47.1° from nadir
2 = 47.1°-50.7° from nadir
3 = 50.7°-53.8° from nadir
4 = 53.8°-56.8° from nadir

Moisture ranges: m_1 = average moisture in the top 0-1 cm, cm^3/cm^3
m_3 = average moisture in the top 0-3 cm, cm^3/cm^3
m_5 = average moisture in the top 0-5 cm, cm^3/cm^3
m_9 = average moisture in the top 0-9 cm, cm^3/cm^3
m' = effective moisture content in 1/2 skin depth, cm^3/cm^3

s = slope of linear least-square fit
r = linear correlation coefficient

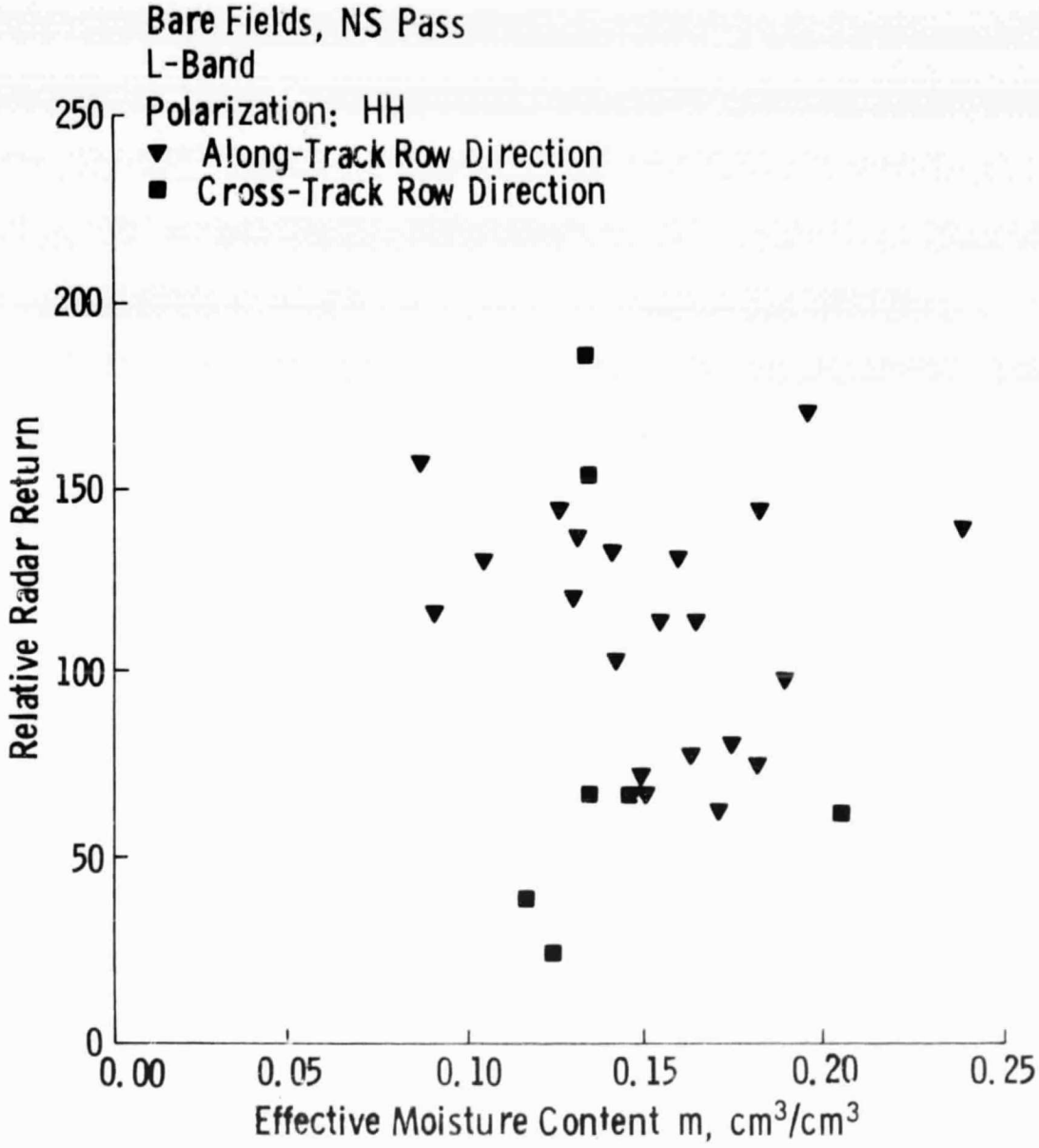

Figure 16. L-band relative HH return as a function of moisture content for fields with row direction along (▲) and cross (■) relative to the flight direction.

these classes (Figure 17). The scatter of the data points belonging to each of the four classes preclude establishing ridge height as the primary interferring factor. The effect of ridge height was also poorly defined for all four classes in the case of L_{HV} return.

Another measure of surface roughness extracted from the photographic records of the thin plate profiles was micro-roughness, defined as the average size of soil surface undulations due to clods of soil material. The overall range between 0 and 15 cm was divided into four categories: 0-1.25 cm, 1.25-2.5 cm, 2.5-3.75 cm, and 3.75-5.0 cm. R_L(HH) data points plotted on previous graphs were allocated to these categories as shown in Figure 18. No consistent relationship between points from the same class is apparent, thus suggesting that the micro-roughness was not an important parameter in this data set.

6. SUMMARY

Using L-band and X-band dual-polarized measurements acquired by the ERIM radar system, an attempt was made to determine the relation between radar backscatter and soil watern content of bare and vegetated agricultural fields. In spite of serious data limitations, positive linear relationship between L-band radar return and soil moisture was established for a small set of fields with similar angles of incidence.

In future experiments, efforts should be made to generate accurate data so that conclusions of controlled ground-based measurements (Ulaby, 1974; Ulaby et al., 1974) could be verified and/or built upon. Specifically, it will be necessary to acquire radar measurements a) at angles of incidence closer to nadir than is presently possible with the ERIM system, b) with calibrated scatterometers or imagers with known antenna patterns, and c) over a wider range of soil moisture contents.

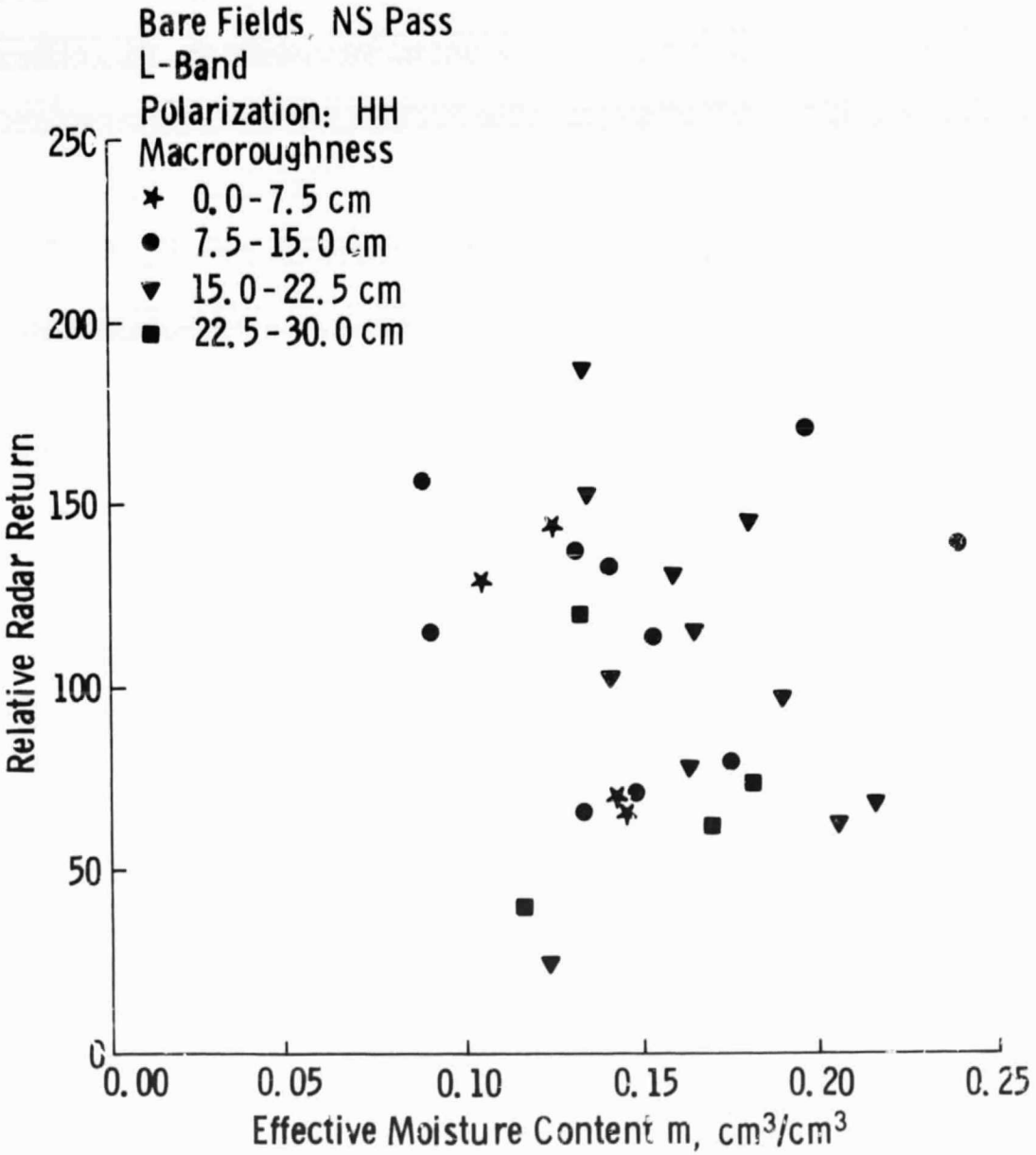

Figure 17. L-band relative HH return as a function of effective moisture content. The fields are divided into different groups based on their macroroughness.

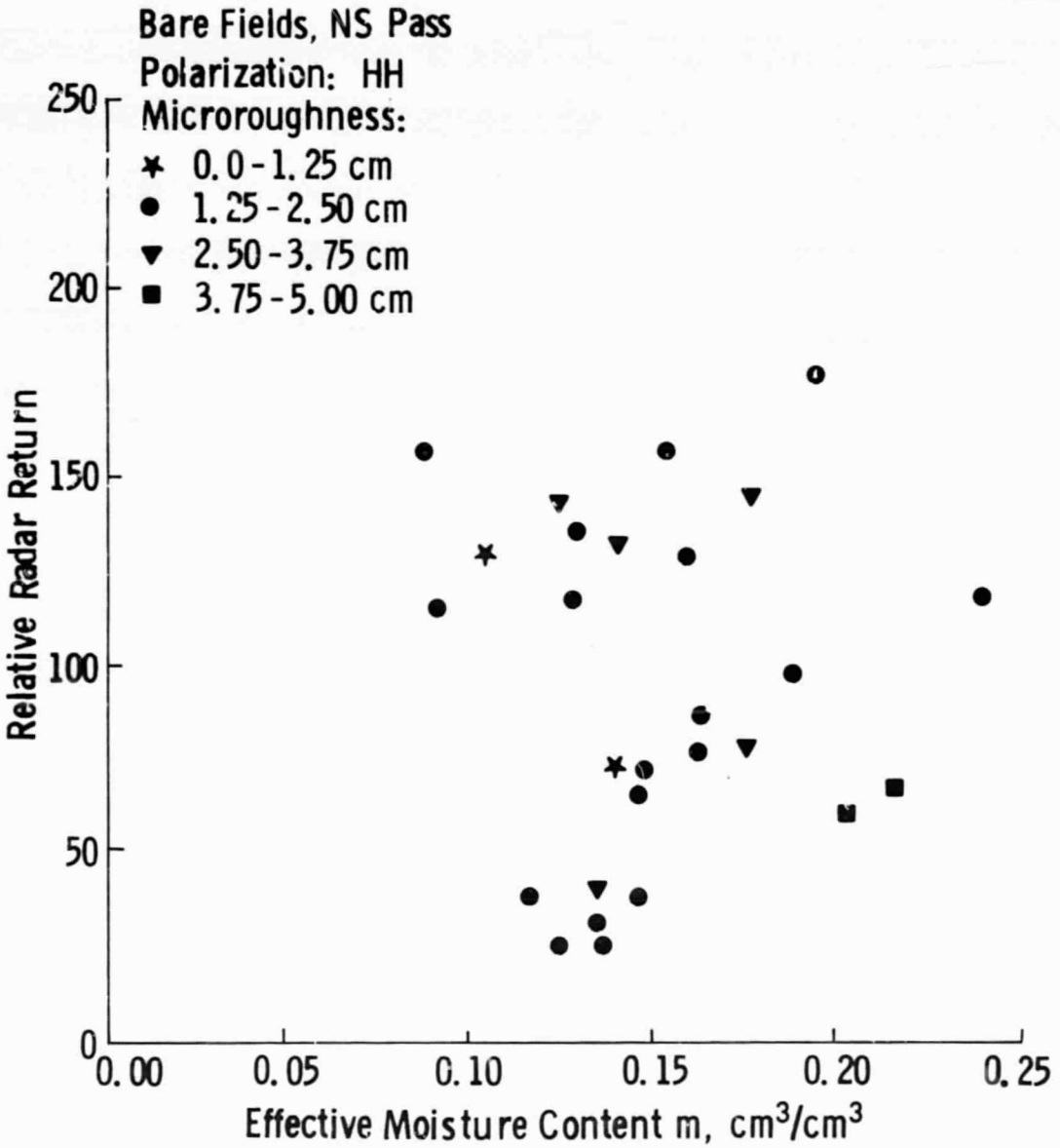

Figure 18. L-band relative HH return as a function of effective moisture content. The fields are divided into different groups based on their microroughness.

REFERENCES

Batlivala, P. P. and J. Cihlar, "Joint Soil Moisture Experiment (Texas): Documentation of Radar Backscatter and Ground Truth Data," RSL Technical Report 264-1, University of Kansas Center for Research, Inc., Lawrence, Kansas, April, 1975.

Blanchard, B. J., "Soil Moisture Data Report, Phoenix Microwave Experiments," ARS-SM-74, United States Department of Agriculture, Chickasha, Oklahoma, September, 1974.

ERIM (Environmental Research Institute of Michigan), "Radar Data Processing and Analysis: Final Report," Ann Arbor, Michigan, 1975.

Rawson, R., and F. Smith, "Four Channel Simultaneous X-L Band Imaging SAR Radar," Proc. Ninth Intl. Symp. on Remote Sensing of Environment, vol. 1, pp. 251-270, April, 1974.

Ulaby, F. T., "Radar Measurement of Soil Moisture Content," IEEE Transactions on Antennas and Propagation, vol. AP-22, no. 2, pp. 257-265, March, 1974.

Ulaby, F. T., J. Cihlar and R. K. Moore, "Active Microwave Measurement of Soil Water Content," Remote Sensing of Environment, vol. 3, pp. 185-203, 1974.